Teknillinen korkeakoulu
Materiaalitekniikan osasto
Metalli- ja materiaalioppi

Masters Thesis
Conducting, transparent and flexible carbon nanotube thin films

Abstract

Author, Name of the Thesis **Jussi Heikkonen** **Conducting, transparent and flexible carbon nanotube thin films**	
Department **Materials science and engineering**	Professorship **Physical Metallurgy and Materials Science**
Supervisor **Professor Ari Lehto**	Instructors **Professor Esko Kauppinen, PhD David Brown**

The relatively new field of electronics is carbon nanotube based electronics. The subject of this thesis is a new branch in the field of transparent electrodes. This thesis describes the process of manufacturing transparent, flexible and conducting layers based on carbon nanotubes and studies their properties. The demand for such material is based on the fact that the materials used commercially, transparent conducting oxides, are costly, availability is poor and they are rather complicated to manufacture.

In the theory part of the thesis, the history and basic properties of carbon nanotubes are presented. The difference between different types of carbon nanotubes is distinguished. The synthesis methods for carbon nanotubes are described in detail. The properties of carbon nanotube thin films are described in detail, focusing on the two key properties that are sheet resistance and transparency. The theory part also describes the common manufacturing methods for carbon nanotube thin films and presents methods for fabricating applications that are using these thin films.

In the experimental part, the used methods and equipment used are presented. The two key properties of the thin films are studied using various processing and modification steps. The sheet resistance behavior is studied via percolation theory. Carbon nanotube based thin film fabrication and modification, in ambient temperature are presented step by step in detail.

The results part of the thesis presents the achieved results. The results are comparable to other published results considering the two key properties. Future work in this field of carbon nanotube electronics is discussed.

Tiivistelmä

Tekijä, työn aihe (suomeksi) **Jussi Heikkonen** **Sähköäjohtavat, läpinäkyvät ja taipusat hiilinanoputki ohutkalvot**	
Osasto **Materiaalitekniikka**	Pääaine **Metalli- ja materiaalioppi**
Valvoja **Professori Ari Lehto**	Ohjaajat **Professori Esko Kauppinen, Fil. tri. David Brown**

Elektroniikan uusimpiin alueisiin kuuluu hiilinanoputkiin perustuva elektroniikka. Tämän työn aihe on uusi haara läpinäkyvien elektrodien alueella. Tämä työ kuvailee hiilinanoputkiin perustuvien läpinäkyvien, johtavien ja taipuisien kerrosten prosessi- ja valmistusvaiheet ja tutkii niiden ominaisuuksia. Tämän tyyppisen materiaalin kysyntä perustuu nykyisten kaupallisten materiaalien, kuten läpinäkyvien johtavien oksidien, kovaan hintaan, saatavuuteen ja hankaliin valmistusvaiheisiin.

Työn teoriaosassa käydään läpi hiilinanoputkien historia ja tavallisimmat ominaisuudet. Erityyppisten hiilinanoputkien ero tehdään selväksi. Hiilinanoputkien synteesi esitetään yksityiskohtaisesti. Hiilinanoputki ohutkalvojen ominaisuudet esitellään, keskittyen kahteen pääominaisuuteen jotka ovat pintajohtavuus ja läpinäkyvyys. Teoriaosa esittää myös hiilinanoputki ohutkalvojen yleisimmät valmistustavat ja kuvailee hiilinanoputki ohutkalvoja käyttävien sovellusten valmistusta.

Tutkimusosa käsittää käytetyt menetelmät ja laitteiston. Kahta pääominaisuutta tutkitaan useilla eri prosessi- ja muokkausvaiheilla. Pintajohtavuutta tutkitaan perkolaatioteorian avulla. Huoneenlämmössä tapahtuva Hiilinanoputki ohutkalvojen valmistus ja muokkaus esitetään askel askeleelta yksityiskohtaisesti.

Tulososassa esitetään saadut tulokset. Tulokset ovat hyvin verrattavissa muihin julkaistuihin tuloksiin ajatellen kahta pääominaisuutta. Hiilinanoputki ohutkalvoihin liittyvistä tulevista töistä mainitaan.

Foreword

This Thesis was made in the Laboratory of Physics in the Helsinki University of Technology in the year 2007.

I would like to thank everybody in the NanoMaterials Group for a nice working environment. Special thank you goes to my instructor, Professor Esko Kauppinen, for the opportunity to work on this project and for a very interesting subject. I would also like to thank my second instructor Dr. David Brown for guiding and teaching me for six months, Dr. Albert Nasibulin for useful information, Anton Ansimov, Prashanta Reddy, and Janne Raula for guidance and helping me with my measurements.

Also a special thank you goes to my precious family and friends.

Table of contents

1 Introduction

This master's thesis researches the processing and properties of carbon nanotube thin films. The carbon nanotubes have been under a serious research for the last 15 years, and no signs of slowing down are seen. The carbon nanotube thin films are just a branch of research areas related to carbon nanotubes. The carbon nanotube thin films require high electronic performance, flexibility and optical transparency. The applications using carbon nanotube thin films are considered to be flat panel displays, touch screens, thin film transistors, photovoltaic devices and much more.

This thesis describes the processing of the carbon nanotube thin films all the way from the carbon nanotube synthesis to the finished product that is a conducting, transparent and flexible carbon nanotube thin film on a polymer substrate. The thin film consists of a network of different types of carbon nanotubes that are bundled together to form a spider web-like conducting network. The low density networks take advantage of the excellent electronic, mechanical and thermal properties of single walled carbon nanotubes. The transparency of the networks can be higher than 90 %. The carbon nanotube thin films are considered as novel alternative for current choice of material for transparent electrodes such as semi-conducting metal oxides and conducting polymers. Background information for the thesis was gathered from books and published articles that are available in large amounts.

The future looks bright for carbon nanotube thin films and carbon nanotube applications in general. Lots of research is done all around the world by research groups and companies as the interest for the subject is both fundamental and industrial. The commercialisation of applications using carbon nanotube electronics is just a few years ahead according to most optimistic estimates.

2 History

Carbon nanotubes (CNTs) were first introduced to the world in 1991 by Sumio Iijima, when he reported that he had found a finite carbon structure consisting of needle-like tubes [1]. The needle-like tubes were produced using an arc-discharge evaporation method that was generally used for fullerene synthesis. The needle-like tubes were in fact multi-walled carbon nanotubes (MWCNTs) ranging from a few to a few tens of nanometer in diameter [1]. It took almost two years of researching when Iijima and Donald Bethune synthesized the first single-walled carbon nanotubes (SWCNTs) [2]. In between 1991 and 1993 MWCNTs were studied at large scale and enthusiasm. It was discovered that the CNTs were conducting, and it was proposed that the tubes were metallic [3]. The structure of the nanotubes was also under research and it was reported that the tube strength of the nanotubes exceeded the highest values found in presently available materials [4]. After the mid 90′s the research of carbon nanotubes has grown. The research has been done all over the field of CNTs e.g. synthesis, electronic properties, structural properties and application properties to name few. Figure 1 shows the remarkable growth of publications and patent applications per year.
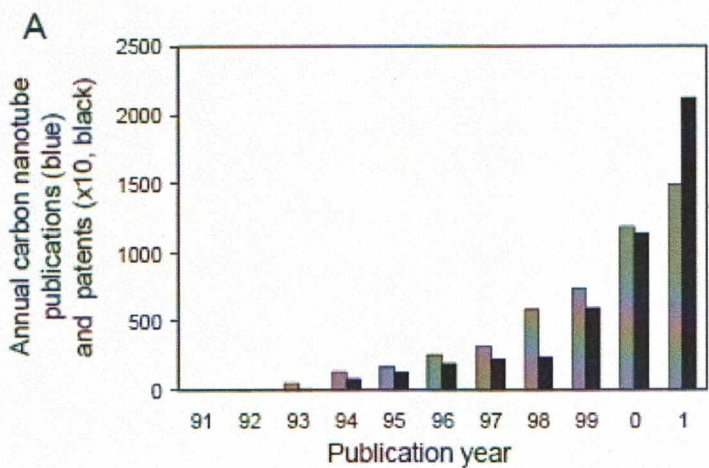

Fig. 1. Comparison of the annual number of scientific publications with the number of patent filings and issuances for the carbon nanotube area [5]

3 Structural properties of carbon nanotubes

Carbon nanotubes are hollow cylinders that have diameters ranging from 1nm to 50nm depending whether they are single-walled carbon nanotubes or multi-walled carbon nanotubes. They consist of only carbon atoms and therefore can be thought to be as graphene sheet that has been rolled into a seamless concentric cylinder [6]. The difference between SWCNTs and MWCNTs is that SWCNTs consists of just one layer of graphene sheet and MWCNTs consists of multiple SWCNTs within each other [6].

Each SWCNT can therefore be seen as conformal mapping of the 2D lattice of a single graphene sheet [7]. Graphene assumes the form of a 2D sheet of carbon atoms that are arranged in a hexagonal array. Thus each carbon atom has three nearest neighbors [8]. The atomic structure of nanotubes can be described in terms of the tube chirality, which is described by the chiral vector $\vec{C}_h$ and the chiral angle θ as seen in figure 2. The chiral vector can be described with two unit vectors $\vec{a}_1$ and $\vec{a}_2$, and two integers n and m as seen in equation (1).

$$\vec{C}_h = n\vec{a}_1 + m\vec{a}_2 \qquad (1)$$

In equation (1) the integers n and m are the number of steps along the carbon bonds of the hexagonal lattice.

If we take a look at figure 2 and roll the graphene sheet along the dotted lines so that the tip of the chiral vector touches the tail of the vector we can visualize the structure of a SWCNT [8].
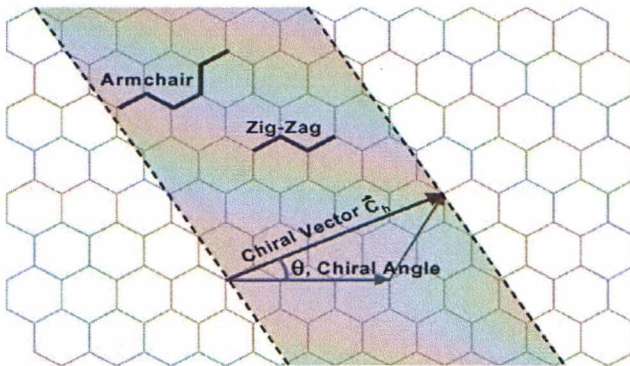

Figure 2. Schematic diagram of a hexagonal graphene sheet [8].

There are also two limiting cases shown in figure 2. When the chiral angle is 0° and the integers are (n, m=n) the nanotube is called *armchair* tube and when the chiral angle is 30° and integers are (n, m=0) the nanotube is called a *zigzag* tube. Whenever the chiral angle is between 0° and 30° the nanotube is simply called *chiral* tube [9]. Thus chiral angle is the factor that determines the twist of the nanotube. The chirality of the CNT has a strong influence on the properties of the tube and it will be discussed more detailed later on this thesis. The three possible chirality forms for SWCNTs are presented in figure 3.
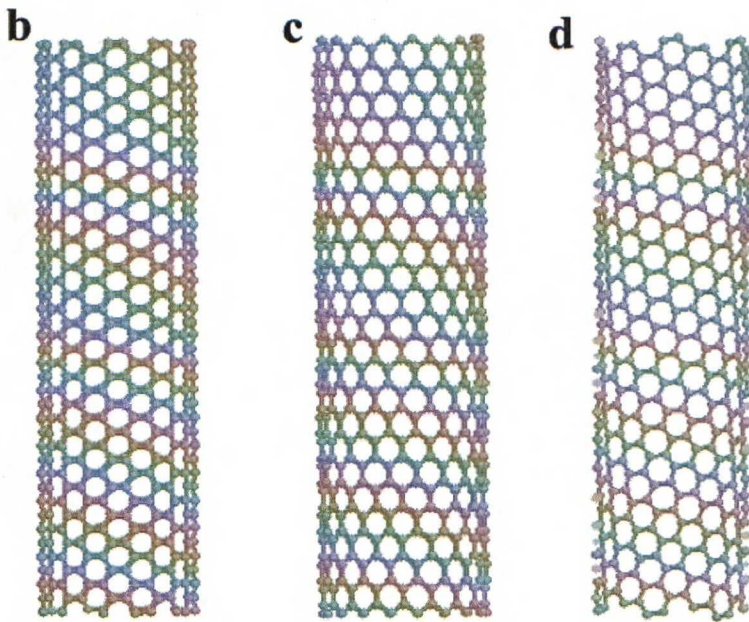
Figure 3. Three forms of chirality. B is *armchair* tube, C is *zigzag* tube and D is *chiral* tube [10].

The carbon nanotubes can either be open ended or they can have a cap at each end. The caps at the end are cylindrical, so that they form a fullerene when joined together [9]. The carbon – carbon distance i.e. carbon bond length in the hexagonal is 1,421 Å [9]. The diameter of an individual CNT depends on the integers n and m, the larger the integers, the larger the diameter. The smallest diameter of a CNT is expected to be below 4 Å (0,4 nm), because a fullerene C_{20} is the smallest possible cap that has the

hexagons and pentagons to fit the CNT [11]. The length of SWCNTs is usually a few hundred micrometers, although nanotubes up to 4cm have been reported [12].

This thesis focuses on flexible thin films, which require a high electronic conductivity, flexibility, strength and optical transparency. In structural sense, this means that the CNTs must form a conducting network of SWCNT that are more transparent than MWCNTs, because of the less scattering they cause when light passes through. The network should be dense enough to form pathways that have metallic conductivity throughout the network, but still sparse enough to be highly transparent. The flexibility and high strength are a cause of the spider web-like form of the network [13].

4 Mechanical properties of carbon nanotubes

The small diameter of a carbon nanotube gives the tube an advantage against e.g. micro-scale fibers. The most appealing mechanical effect of the small diameter is the opportunity to associate high flexibility and high strength with high stiffness, a property that is absent in graphene sheets [14]. The mechanical properties of CNTs have mostly been studied on theoretical level rather than experimental level, due to the challenge in manipulating nanometer size objects. However, development in instrumentation, especially high-resolution transmission electron microscopy (HRTEM) and atomic force microscopy (AFM) are giving more and more experimental results on the properties of CNTs [14].

Young's modulus of a material is the key coefficient defining the elastic properties of a material. In practice, structural engineering is largely based on elasticity, and designing of a material/product is concerned with stresses below the elastic limit [12]. The theoretical Young's modulus given in literature [2] for SWCNT is ~1 TPa. The experimental value achieved is also around 1 TPa [2]. This is the also case for MWCNTs. For ropes of SWCNTs, or bundles in other words, the Young's modulus is 0,4 – 0,8 TPa [2]. For comparison, wrought steel reaches values of less than 200 GPa [15], so a single carbon nanotube provides five times higher Young's modulus. Especially the density of carbon nanotubes, which is 2,6 g/cm^3, is intriguing compared to the density value of steel, 7,8 g/cm^3 [15, 16]. With such high modulus and low density, future structural applications are more than interesting, considering e.g. weight reduction and related.

Carbon nanotubes are very robust and can handle significant deformations without losing their properties. This property is a significant advantage designing applications that are flexible and still need, for example, electronic conductivity. This thesis focuses on the electronic properties of carbon nanotube networks that are deposited on flexible substrates, thus this property of CNTs is going to be under specific research.

6

5 Thermal properties of carbon nanotubes

Thermal properties of carbon nanotubes are important to know, especially when they are used in nanoscale electronic devices, where predicting the thermal transport properties of compounds is crucial considering the reliability of the device [17]. Diamond is a carbon based material, with the highest observed value of thermal conduction 41 000 W/mK. This is due to the highly stiff sp^3 bonds. Since carbon nanotubes have even stronger sp^2 bonds, a high thermal conductivity is also expected. Berber et al. [17] have shown that a single carbon nanotube yields thermal conductivity as high as 37 000 W/mK, and a room temperature value of 6000 W/mK. Figure 5 shows the measured thermal conductivity values compared to temperature, by Berber et al [17]. The given values are extremely high and can be compared to pure diamond. However when CNTs are in the form of bundles and networks, the thermal conductivity decreases dramatically. The decrease can be compared to the electronic conductivity of CNT networks, as they are also lower than the electronic conductivity values for a single carbon nanotube [18]. The reported value for as grown carbon nanotube networks by Hone et. al. is only 35 W/mK [18].
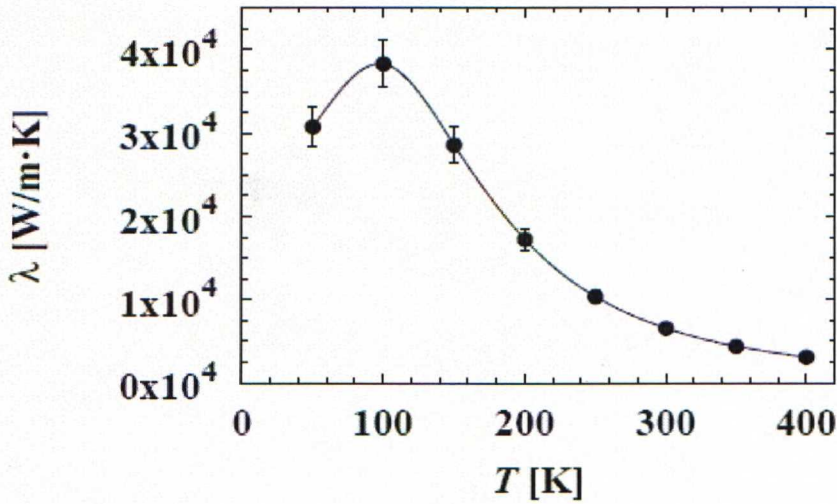

Figure 5. Thermal conductivity of a single CNT vs. temperature [16].

6 Electronic properties of carbon nanotubes

Although carbon nanotubes exhibit various extremely intriguing and superior properties, the electronic properties are probably the most intriguing and researched properties of them all. As electronic devices and components become smaller and smaller, certain limitations to existing materials and applications are starting to rise up. Many people think and wish that nanoscale materials as building blocks are the solution to these problems. This thesis is also focused on the electronic properties of carbon nanotubes and more importantly electronic properties of CNT thin films, so this chapter is approached with more detail. As for the transparent CNT thin films, it has been shown that SWCNTs are more suitable because they scatter less light than MWCNTs and are therefore more transparent, so we will concentrate on the electronic properties of just SWCNTs [19].

The most exciting thing about the electronic properties of SWCNTs is that they can be either metallic conductors or semiconductors. This property as well as the diameter and helicity of the tubes, is uniquely characterized by the chiral vector from equation (1) [20]. Electronic band structures of SWCNTs have been studied and it has been shown that the integers *n* and *m* determine the conducting behavior of SWCNTs. Zigzag (n, 0) type SWCNTs are expected to metallic, when n/3 is an integer, and in any other case semiconductor. Chiral (n, m) SWCNTs are metallic when (2n + m)/3 is an integer, and in any other case semiconductor. Armchair (n, n) SWCNTs are expected to be truly metallic in every case. The band gaps of the semiconductor type tubes are approximately inversely dependent of the radius of the tubes [20]. With the preceding data, we can conclude that in a random sample of SWCNTs about 1/3 of the possible SWCNTs are metallic and 2/3 are semiconductors. This is a unique attribute among the known materials in the world, and SWCNTs are considered as promising building blocks of a future nanoelectronic technology. Researchers say that, many problems that silicon technology is or will be facing, are not present in carbon nanotubes [21]. Avouris et al. have listed five of important properties of SWCNTs considering electronics, in 2003 [21]:

1) Carrier transport is 1D. This implies a reduced phase space for scattering of the carriers and opens up the possibility of ballistic transport. Correspondingly, power dissipation is low. Furthermore, their electrostatic behavior is different from that of silicon devices with implications on screening and electron/hole tunneling.

2) All chemical bonds of the C atoms are satisfied and there is no need for chemical passivation of dangling bonds as in silicon. This implies that CNT electronics would not be bound to use SiO_2 as an insulator. Instead high dielectric constant and crystalline insulators can be used, allowing, among other things, the fabrication of 3D structures.

3) The strong covalent bonding gives the CNT high mechanical and thermal stability and resistance to electro migration. Current densities as high as 10^9 A/cm^2 can be sustained.

4) Their key dimension, their diameter, is controlled by chemistry, not conventional fabrication.

5) In principle, both active devices (transistors) and interconnects can be made out of semiconducting and conducting nanotubes, respectively.

To understand the electronic properties of SWCNTs, the tube can be thought as a graphene sheet that has been rolled up into a cylinder. Consequently, the electronic properties can be directly derived from the electronic properties of graphene, with unique characteristics resulting from the arrangement of the carbon atoms of the rolled up graphene sheet. The rolling of graphene sheet, thus the geometry of the tube, can also be described with the chiral vector that was given in equation (1) [2]. The intriguing electrical properties of SWCNTs are due to the unique electronic structure of the graphene. Figure 6a shows the band structure and first Brillouin zone of graphene (bottom). The Brillouin zone is the reciprocal lattice of a primitive cell and it could be defined as the set of points in **k** space that can be reached from the origin without crossing any Bragg plane. The energy surfaces in the figure 6a are valence (π) and conduction (π^*) states, that degenerate at six K points (Fermi points) lying at the Fermi level [21]. The density of the states is zero at the Fermi level, so 2D graphene sheet is a zero-bandgap semiconductor.
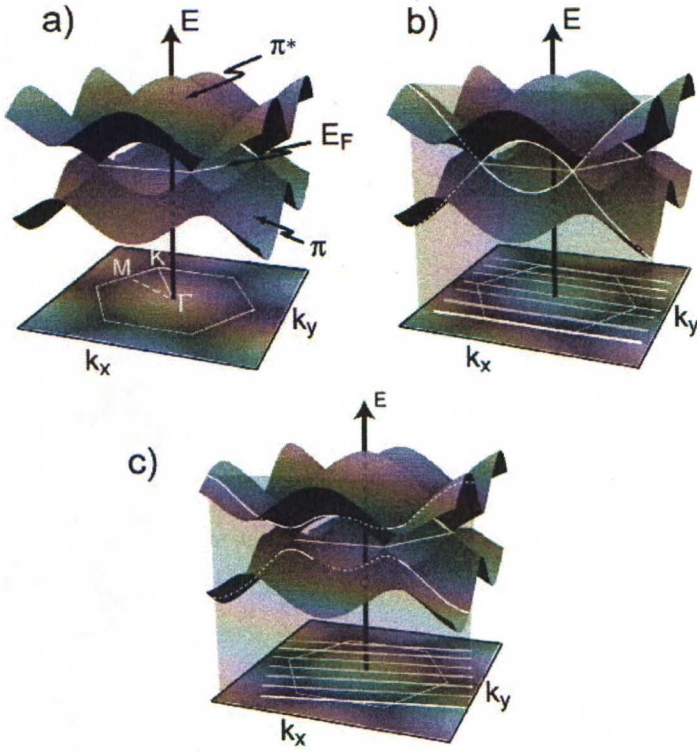
Figure 6. (a) Band structure of a graphene sheet (top) and the first Brillouin zone (bottom). (b) Band structure of a metallic (3, 3) CNT. (c) Band structure of a (4, 2) semiconducting CNT. The allowed states in CNTs are cuts of the graphene bands indicated by the white lines. If the cut passes trough a K point, the CNT is metallic, otherwise semiconducting [21].

In figure 6b the states of a metallic (3, 3) SWCNT are shown. The metallic behavior can be explained with the band structure. The allowed energy states are cuts of the graphene band structure and when they cut pass through a Fermi point, as in figure 6b the tube is metallic. Figure 6c shows the band structure of a semiconducting SWCNT. As can be seen from the figure, no cut passes the K point, thus the semiconducting behavior and the band gap seen between the valence and conduction bands [21]. It is seen from figure 6c that the semiconducting SWCNTs have a direct bandgap, which enables the emission of light. As stated before the band gap of semiconducting SWCNTs is approximately inversely proportional to the tube diameter. Due to the tight-binding description of the electronic structure, the band gap E_{gap} is given by equation (2) [2].

$$E_{gap} = \gamma(2a/\sqrt{3}d_{CNT})$$

(2)

In equation (2), γ is the hopping matrix element, $a = \sqrt{3}d_{C-C}$, with d_{C-C} is the carbon-carbon distance, and d_{CNT} is the tube diameter.

Metallic SWCNTs have a two-terminal conductance, which is determined by Landauer-Buttiker formula for 1D conductors, and is given in equation (3)

$$G = (2e^2 / h) \cdot \Sigma_i^N T_i \qquad (3)$$

In equation (3) $2e^2 / h$ is the quantum unit of conductance, and T^i is the transmission of the ith conducting channel [2]. When there is no scattering involved in the conductance, i.e. $T^i = 1$, a metallic nanotube has a resistance $R = 1 / G = h / (4e^2) \approx 6,5 \ k\Omega$, because there are two conducting channels near the Fermi energy [2, 20]. Transport in metallic SWCNTs at low energies is considered ballistic, i.e. no scattering, over distances of a micron or so [2].

7 Carbon nanotube synthesis

The Nano Materials Group (NMG) in Helsinki University of Technology (HUT) laboratory of physics is using different synthesis methods to produce CNTs. The synthesis methods are based either aerosol or chemical vapor deposition (CVD) synthesis processes. The three synthesis methods used are ferrocene and iron decomposition method, hot wire generator (HWG) method, and a substrate CVD method. Other methods for CNT synthesis are also available, including laser ablation method, arc discharge method and high pressure carbon monoxide process (HipCO) that are widely used by researchers and manufacturers around the world. The next sections reveal the basics of the synthesis methods used in NMG.

7.1 Ferroscene and iron decomposition method

The following exposition of theory is entirely based on the reference [22] by Moisala et al.

This CNT synthesis method is a gas-phase CVD method, which uses ferrocene or iron pentacarbonyl as catalyst nanoparticles for carbon source decomposition as well as CNT formation sites. The carbon source should ideally decompose only at the surface of the catalyst nanoparticles, and that way liberate the carbon atoms for CNT formation. Many carbon sources such as hydrocarbon and alcohols thermally self-decompose at high temperatures. This results in the formation of unwanted by-products such as amorphous carbon and soot particles. This can be avoided using carbon monoxide (CO), because the reaction $2CO(g) \leftrightarrow C\ (s) + CO_2(g)$ requires the presence of a catalyst surface.

In this gas-phase CVD method, controlling the conditions for CNT growth are able to do by observing the temperature conditions and the location at the reactor. These factors affect the SWCNT length, and the sizes of catalyst particles subsequently determine the formation of the CNTs. The SWCNTs are produced via thermal decomposition of ferrocene or iron pentacarbonyl in the presence of CO. To be able to measure the temperature and the SWCNT growth rate in situ sample collection method can be used.

The vertical laminar flow reactors are shown in figure 7. The set-up includes a precursor feed system, a furnace equipped with an alumina tube and analysis devices. Carrier gases, nitrogen (N_2, 99,999 vol %), nitrogen/hydrogen mixture (N_2 / H_2, 93/7 vol%, AGA) or carbon monoxide (CO, 99,97 vol %) which also served as the carbon precursor, are used.

To be able to vaporize ferrocene ($FeCp_2$, 99 %) a flow of carrier gas (300 cm^3 / min) is continuously directed through a cartridge containing the precursor powder mixed with silicon dioxide powder (99,9 %s, weight ratio $FeCp_2$: SiO_2 = 1:4) at ambient temperature. A constant partial pressure of 0,8 Pa of $FeCp_2$ vapor is introduced to the reactor. The flow direction is downward.

Iron pentacarbonyl ($Fe(CO)_5$, 99, 999%) vapor is introduced to the furnace by bubbling a carrier gas (N_2) through a reservoir of the liquid catalyst precursor at ambient temperature. Precursor vapor is introduced 16 – 30 cm from the furnace inlet at the flow rates between 310 – 407 cm_3 / min. The precursor vapor pressure is 0,3 or 4 Pa based on the equilibrium vapor pressure data, taking into account the dilution with N_2 prior to the furnace. The flow direction is upward.
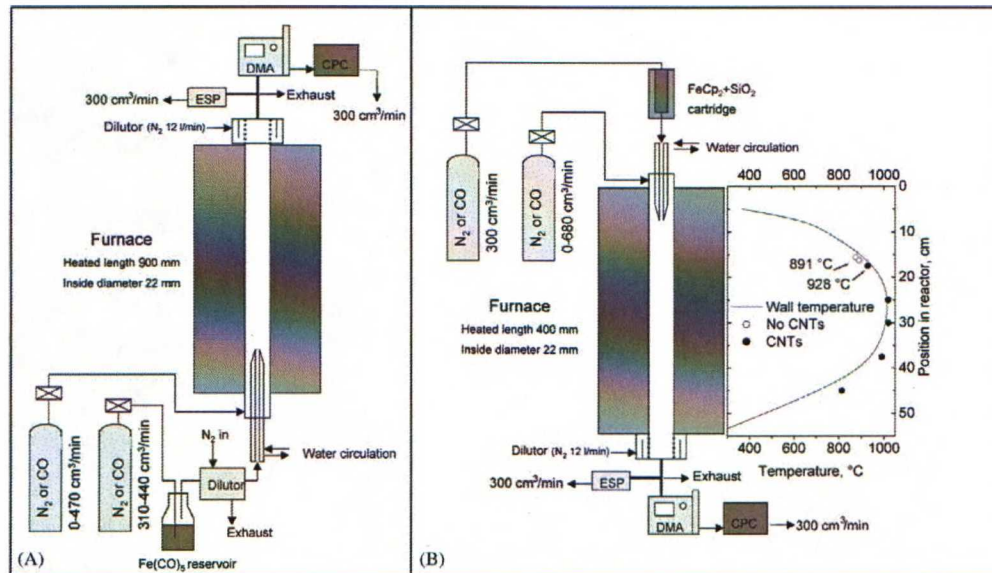
Figure 7. Set-ups for iron pentacarbonyl (A) and ferrocene (B) reactors, with the wall temperature profile and centerline location of the in situ sample collection shown for ferrocene experiments. Open circles represent sampling locations when CNTs were not observed, solid circles show the conditions of the CNT sampling [22].

The precursors are fed to the furnaces through water cooled stainless steel injector probes, which are held constantly at 22 °C. The location of these injector probes

13

can be varied as they control the precursor heating rate and residence time in the furnace. The nanotubes can be collected to a 25mm diameter filter that is located at the outlet of the reactor. The CNTs are in the form of a nanotube network of CNT bundles on the filter, and various types of filters can be used. The in situ sampling from the centerline of the reactor can be carried out to detect the location and the temperature of SWCNT growth. To do so, a silica coated nickel transmission electron microscope (TEM) grid is attached to a stainless steel rod and inserted into a selected location of the furnace for 30s. Samples can also be collected from the gas phase by an electrostatic precipitator on carbon coated copper TEM grids. The carrier gas flow rates are determined by a flow meter and the furnace wall temperature is measured with nichrome-nickel thermocouples. The aerosol mobility number size distributions (NSDs) in the size range of 9,8 – 400 nm can be measured by a differential electrical mobility particle size system. The system consists of a differential mobility analyzer (DMA) and a condensation particle counter (CPC). The DMA system allows to measure the electrical mobility of aerosol particles and thereby to distinguish catalyst particle aggregates from the bundles of CNTs.

In order to provide reproducible SWCNT synthesis conditions the reactor walls have to be saturated with iron. This is achieved by introducing $FeCp_2$ to the heated furnace with N_2 as the carrier gas prior to the introduction of CO. The diameter of the nanotubes provided by this method are from 0,9 nm to 3 nm. The length of the CNT bundles varies from hundreds of nanometers to a few micrometers, depending significantly on the set temperature and residence time. Figure 8 provides a schematic presentation of the SWCNT nucleation from the surface of the catalyst particle.
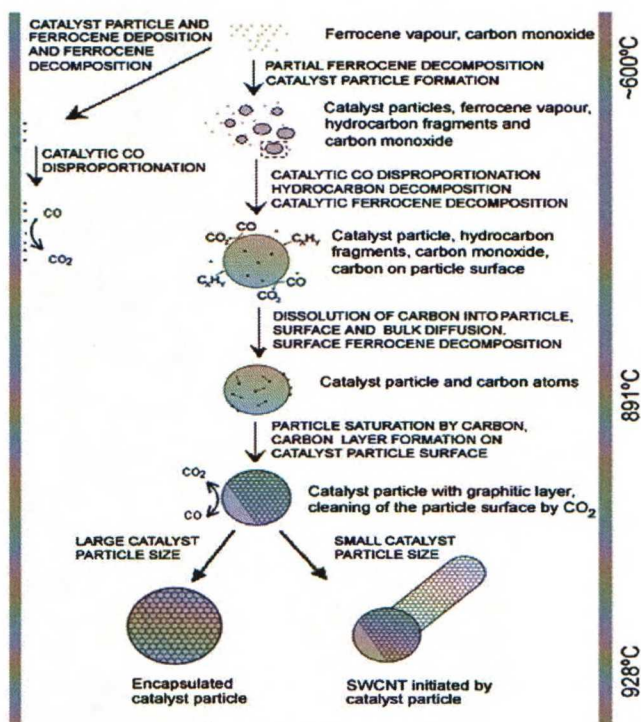
Figure 8. Schematic of SWCNT formation mechanism in FeCP$_2$ set-up with CO as the carbon precursor at temperature of 1000 °C [22].

7.2 Hot wire generator method

The Hot wire generator (HWG) method for CNT synthesis is a novel aerosol method discovered in the NMG at HUT. The following exposition of theory is entirely based on the reference [23] by Nasibulin et al.

The HWG method is an aerosol method that includes the production of catalyst particles by metal vaporization, subsequent particle formation due to nucleation and condensation of the supersaturated vapor, and cluster growth by coagulation, followed by subsequent introduction of the particles into a laminar flow reactor, where suitable conditions for CNT formation are maintained. Iron and CO are used as material precursors for catalyst particle and atomic carbon production.

Figure 9. Schematic of the hot wire generator (HWG) [23].
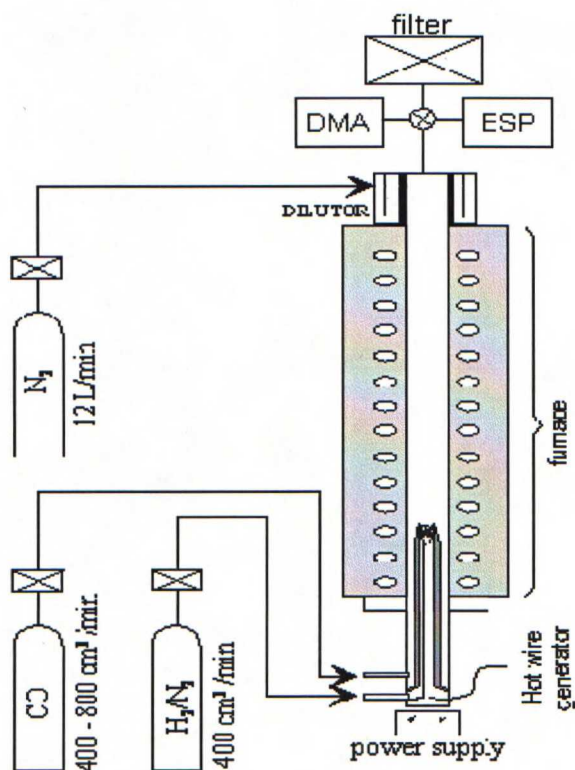
Figure 9 shows a schematic of the laminar flow reactor, which consists of a HWG and a heated vertical tubular reactor. A ceramic tube, which has an internal diameter of 22 mm and is inserted inside the 90 cm length furnace, is been used as a reactor. Inside the reactor is another ceramic tube, which protects the HWG from the CO atmosphere. The HWG itself consists of a resistively heated thin iron wire (0,25 mm in diameter) and it is located inside the inner ceramic tube. The location of the inner tube and the HWG can be adjusted. The metal particles that are produced by the HWG are carried into the reactor with nitrogen/hydrogen (93,0 % / 7,0 %) or nitrogen flows. Inside the reactor, the flow of metal particles is mixed with the outer CO flow and CO disproportionation or hydrogenation takes place on the surface of the metal particles. The inner and outer gas flows are introduced to the reactor at a rate of 400 cm^3 / min. A porous tube dilutor is placed downstream of the reactor to prevent the product deposition on the walls. Same kind of in situ sample collection can be used as described in the previous chapter. Hydrogen (H) has a very important role in the as it prevents the oxidation of the iron wire and the nanosized metal particles. The SWCNTs were

nucleated at temperatures between 870 – 1500 °C. The diameter of the catalyst particles are 1 – 3 nm, while the diameter of formed SWCNTs is from 0,6 to 2 nm. It has been also noticed that when the reactor walls are scratched after a time, there are traces of MWCNTs, which have been grown by CVD method to the reactor walls. Thus the HWG method can be used to yield MWCNTs with varying controlled properties.

7.3 Substrate CVD method

Individual SWCNTs are grown by a CVD method on thin SiO_2 and other high temperature films, using catalyst particles and carbon source, such as iron and carbon monoxide. This method combines the synthesis of aerosol particles with their further utilization as catalyst for substrate CVD production of CNTs. Two different methods can be used, *in situ* and *ex situ*. The following exposition of theory is entirely based on the reference [24] by Queipo et al.

The *in situ* method, also called a continuous process, is developed to avoid intermediate stages for catalyst preparation. In this method, the catalyst particle formation, deposition and synthesis of CNTs takes place inside the reactor in subsequent steps. Catalyst particles are introduced to the reactor at set temperatures of 400 – 600 °C. CO is introduced to the reactor in order to prevent sintering. The carbon prevents additional growth of the particles and thus, controls the particle size and the diameter of the nanotubes. Previously mentioned DMA device is used to measure the synthesis conditions during synthesis.

The produced nanoparticles are deposited to the substrate downstream of the reactor by diffusion. The point C1 in figure 10 shows the point where the deposition takes place at a temperature of 120 °C. The nanotube growth takes place at point G in figure 10. Point C2 in figure 10 is a catalyst particle upstream collection point at a temperature of 400 °C. This is done in order to control the growth and avoid possible losses due to diffusion on the reactor walls. This also avoided the gas-phase growth of CNTs. The deposition to the substrate was performed under an outer flow of N_2 or CO.
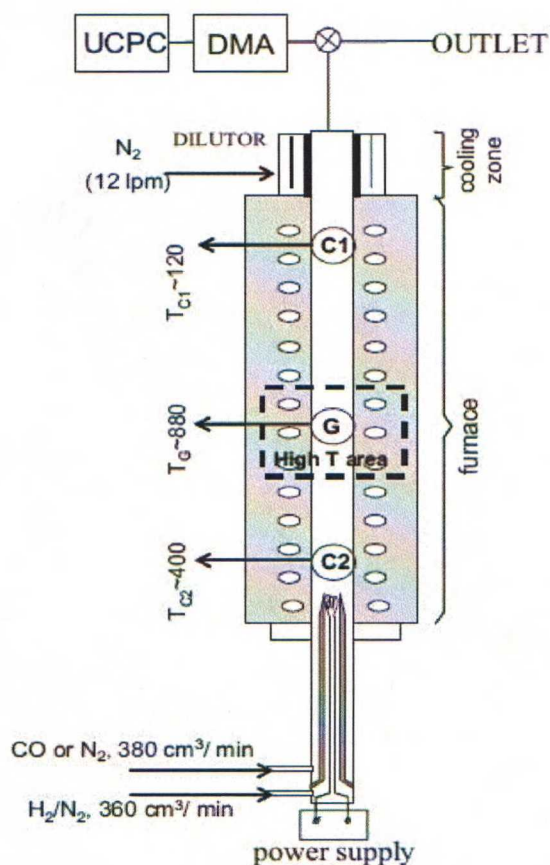
Figure 10. Schematic drawing of the in situ method setup. Points C1 and C2 indicate the areas of the reactor where the catalyst particle collection took place. Point G shows the high temperature zone used for CNT growth [24].

The *ex situ* method, also called a non-continuous method, is also applied to grow SWCNTs. This method provides even better control of the process, especially the deposition of catalyst particles on to the substrate. Thus the catalyst particle synthesis and collecting takes place outside of the reactor. The synthesis uses a HWG and electrostatic precipitator (ESP) as seen in figure 11. Because of the control improvement of the deposition process, more nanotubes can be synthesized. The diameter and length of the nanotubes synthesized are different for *in situ* and *ex situ* method. The first process produces nanotubes with diameters ranging from 2,8 to 6,0 nm, while the length ranging from 3 to 30 µm. The latter process produces nanotubes with diameters ranging from 1,2 to 1,8 nm, while the length being over 50 µm.
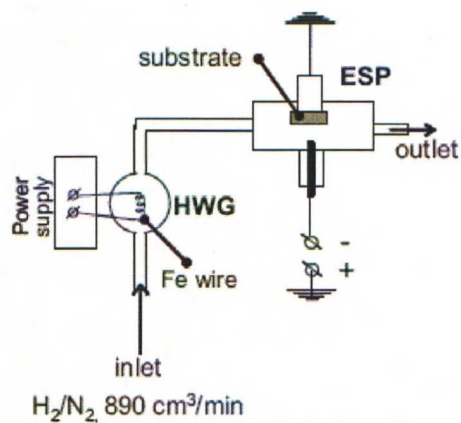
18

Figure 11. **Schematic of the device for the production and collection of the Fe catalyst particles outside the reactor [24].**

Because the particle collection takes place outside of the reactor, the particles can become oxidized and thus inactive for growth of nanotubes. Because of this a higher H_2 concentration is added before and during the growth step.

8 Carbon nanotube thin films

Carbon nanotube thin films can be described as networks that have CNTs, or bundles of CNTs, randomly dispersed in an area. The flexibility of the CNT thin film largely depends on the flexibility of the substrate it is deposited in. Thus if the substrate is flexible the CNT thin film is flexible. This thesis is focused on flexible thin films, so the next chapters will mostly concentrate on properties of these thin films.

8.1 Properties of CNT networks

As stated earlier CNTs have unique electronic properties and as a result they are considered appealing candidates for molecular electronics. Chip miniaturization and attacking the scaling problem of semiconductor devices has already begun with devices based on individual CNTs. However, the difficulty of assembling the individual tubes and the challenge to produce desired chirality for the CNTs still remains a problem [24]. As well the CNT networks have the problem of chirality and geometry, thus current synthesis methods produce CNTs with distributed qualities and so they can be either metallic or semiconducting. In CNT networks however, such effects due to the individual variations are suppressed by the fact that they contain large number of CNTs. Therefore CNT networks can be reproducible and mass produced at low cost and high efficiency [26].

CNT networks have similar properties with individual SWCNTs. They have excellent properties with low sheet resistance and high transparency that are the most important properties when considering transparent and conducting thin films. They also have shown good robust mechanical flexibility and thermal stability [27]. Considering these properties and their use as a transparent conductor in multiple applications they possess qualities comparable to traditional transparent conductors such as Sn doped In_2O_3 (Indium tin oxide, ITO) [27]. For this thesis, the most important properties for CNT thin films are sheet resistance and transparency of the films, so the next two chapters go deeper in to these properties.

8.1.1 Sheet resistance

The conductivity of CNT networks is usually expressed as sheet resistance. Sheet resistance is comparable to the dc resistance by equation 4.

$$R = \frac{\rho}{t}\frac{L}{W} = R_s \frac{L}{W} \Rightarrow R_s = \frac{\rho}{t} \tag{4}$$

In equation 4, R is the dc resistance, R_s is the sheet resistance, ρ is the resistivity, W is the width, L is the length and t is the thickness of the film. The resistance values can be easily converted to conductance values, if needed, as conductance is the reciprocal of resistance, e.g. sheet conductance is $1/R_s$ and conductivity is $1/\rho$.

The sheet resistance is a combination of many aspects of the network, and the hardest task is optimizing them all to get the sheet resistance as low as possible, while maintaining high transparency, which is necessary for high quality thin films. The heterogeneous distribution of the SWCNTs from synthesis means, that the CNT networks electronic properties are highly dependent on the length and diameter of the bundles and from the chirality of the CNTs [25]. The chirality of the CNT determines whether the CNT is metallic or semiconducting, thus having a direct effect on the conductivity. The diameter of the bundle affects the resistance so, that when it is small, the resistance is small. This yields from the fact that the current flows at the surface of the bundles and the inner tubes do not contribute much to the conducting process [28]. The affect of the length of the SWCNT bundles can be described as follows. A SWCNT thin film is comprised of two sources of resistance, the resistance along the individual SWCNT R_{NT}, and the resistance due to the tube to tube junctions in the thin film R_{jct}. It has been shown that the SWCNT networks have $R_{jct} \gg R_{NT}$, thus the network resistance is dominated by the resistance due to the junctions of SWCNT bundles. This leads on to the lower resistance of networks consisting of longer tubes or bundles, because then there are less tube to tube junctions across the thin film area [29]. Hecht et al. in reference 29 have proposed that the sheet resistance of the network can be expressed with as power law dependence with equation 5, where σ_{dc} is the conductivity of the network, which can be directly calculated from the sheet resistance.

$$\sigma_{dc} \approx L_{av}^{\beta} \tag{5}$$

In equation 5, L_{av} is the average length of the CNT bundle and β is an exponent between 0 and 2,48 [29]. Hecht et al. have measured the exponent to be 1,46 in their research case, which in their case hold up 20 – 30 µm long CNT bundles. After that, they have stated that the tube itself comes comparable to the resistance of the junctions, thus a further increase in the CNT bundle length have a limited effect on the sheet resistance [29].

In recent years the sheet resistance, usually expressed as conductivity σ (=1/ρ) in this context, of the SWCNT thin films has been shown to be strongly related to the percolation theory [26]. The density dependence of the conductivity in the SWCNT networks can be expressed with the percolation theory. Thus the conductivity of the networks can be expressed with a certain critical density p_c of the film i.e. the percolation threshold. The continuity of the conductivity of the network is satisfied when the density p is bigger than p_c. When the density is lower than p_c there is not enough conducting pathways, i.e. the network is too sparse to get the whole network conducting [30]. The basic idea of the percolating theory in SWCNT networks is presented in figure 12, where the gray lines represent conducting pathways through the network, as the network is above the critical density i.e. the percolation threshold.
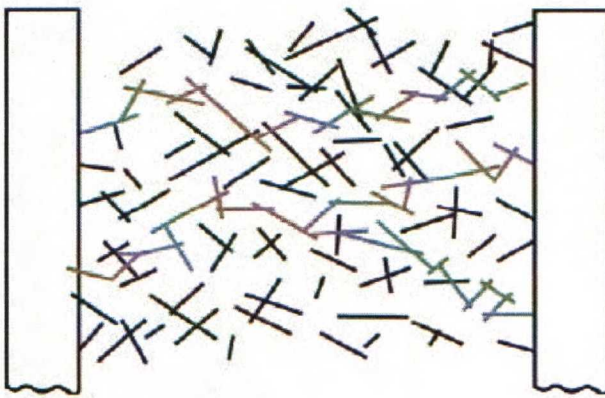

Figure 12. The basic idea of a percolating SWCNT thin film [13].

George Grüner and his group [26, 28] have stated that the SWCNT networks are not conducting until a certain threshold which is denoted in equation 5.

$$l\sqrt{\pi p_c} = 4{,}236 \qquad\qquad (6)$$

In equation 6, p is the density, l is the length and p_c is the critical density of the SWCNT bundles. Above the percolating threshold the conductivity can be expressed with equation 7.

$$\sigma \propto (p - p_c)^\alpha \qquad\qquad (7)$$

In equation 7, α is the critical exponent that depends on the dimensionality of the network, thus it is different for 2D and 3D systems. For 2D films the critical exponent is in theory 1,33 and for 3D films 1,94 [26]. The SWCNT networks are usually considered as 2D thin film, though they are not perfectly two dimensional and some crossover to three dimensions can be seen. The theory also does not take account the fact that the SWCNT network consists of metallic and semiconducting tubes. Thus the nanotube junctions can be metallic-metallic, semiconducting-semiconducting and metallic-semiconducting. The latter is shown to be less conducting due to the schottky barrier [26]. Above the percolation threshold i.e. at higher densities, one can assume that all metallic conducting pathways are present, and the sheet resistance of the network decreases [28]. Equation 6 can be expressed also with using the thickness of the nanotube network [25], which is far more suitable for our research equipment and processes. The thickness correlated conductivity above the percolating threshold is given in equation 8.

$$\sigma \approx (t - t_c)^\alpha \qquad\qquad (8)$$

In equation 8 t is the thickness of the SWCNT network, t_c is the critical thickness and α is the same critical exponent as in equation 6. The critical thickness is experimentally shown to be 3 nm [25].

Conductivity near the percolation threshold is highly temperature dependent, yielding information that the excitation process dominates the conductivity. Well over the percolation threshold, the temperature has little effect to the conductivity

[28]. The weaker temperature dependence of the denser, i.e. thicker, networks points out that more and more efficient tube-tube contacts are formed, as the percolation theory suggests [25, 30].

Considering the electronic properties of carbon nanotube thin films, it is important to point out, that the thin films can act as a semiconducting channel and also as a metallic interconnect, depending of the application it is used for [28]. To get the wanted properties to the SWCNT thin film, numerous physical and chemical treatment processes have been developed, e.g. purifying, densifying and doping the films. Some of the processes will be discussed in detail later in this thesis.

8.1.2 Transparency

The other important property of SWCNT thin films is the transparency of the films, which is essential for most of the applications the material is to be used. As stated earlier in chapter 3. The transparency of the films is an important reason SWCNTs are used instead of MWCNTs, since they are practically 1D and scatter less light. The transparency is strongly related to the density i.e. thickness of the film. As a rule of thumb one can say that the denser the thin film, the less it is transparent. However, as the density also strongly affects the sheet resistance of the film, a compromise between transparency and sheet resistance must be made [28].

The transparency can't be seen as dependent on the sheet resistance, because films can have many different sheet resistances although the transparency is the same. The difference in sheet resistance can be explained by the purity degree of the film, doping of the film and other modifications that do not affect the transparency value [28].

9 Processes for fabricating CNT networks

Carbon nanotube thin films can be fabricated in multiple ways. The basic idea is to get a transparent, conducting and flexible SWCNT film on a plastic, or other flexible and transparent, substrate. To achieve this goal research groups and scientists have developed numerous fabricating methods [26]. As stated earlier SWCNT thin films are considered as an alternative to ITO, which is the current choice of such material. SWCNT thin films have significant advantages as they can be fabricated in room temperature and without vacuum conditions, unlike ITO. Some ITO layers can be manufactured also in room temperatures, but they are low in quality. ITO is also a brittle material, thus it cannot be flexed without affecting its properties [28].

It all starts from the need of single walled carbon nanotubes. Double or multi walled tubes can also be used, but the transparency of the films suffers when using them. To create SWCNTs, many synthesis processes have developed and already mentioned in chapter 7. The biggest difference in producing the feedstock, SWCNTs, is the form that the SWCNTs come out of the synthesis reactor. There are basically two options: 1) The SWCNTs are collected as a powder. 2) The SWCNTs are collected directly to a substrate of some kind, as a direct dispersion of randomly aligned SWCNTs. The NanoMaterials Group is using the latter method [22, 23, and 24]. The next step is to deposit the feedstock material to the flexible and transparent substrate either in one step or multiple steps. This phase also has numerous choices of fabrication [26].

The SWCNTs that are collected as a powder from the synthesis reactor usually need more fabrication steps than the SWCNTs that are collected directly to a substrate. First the SWCNT powder is dispersed into a surfactant solution containing some surfactant, e.g. sodium dodecyl sulfate (SDS) [31]. Some groups sonicate and centrifuge the tubes to dissolve and debundle the nanotubes [26]. The concentration of the solution can be easily adjusted by controlling the weight percent of SWCNT powder in the solution. The concentration of the solution defines the thickness/density of the end product. After the solution is ready for further steps, one can directly deposit the solution to the filter with various methods e.g. spraying, spin coating, dip casting, drop-drying from solvent, Langmuir-Blodgett deposition. Some groups use an extra step and

first use a filtration to a porous filtration membrane, where the solution pours through the pores of the membrane and the interconnected nanotube network stays on the membrane. The density of the films can be controlled by not only the concentration of the solution, but with controlling the filtrated volume of the solution. This yields highly homogenous and overlapping network of SWCNTs [26]. After this extra step, the SWCNT network can be deposited to a flexible and transparent flexible substrate by printing methods or some other deposition method [27 and 32]. The substrate may be in some cases coated with a substance that improves the adhesion of the nanotube network to the substrate [31].

According to many articles, fabricating the SWCNT thin film with the powder/solution process is far more common than fabricating the film from directly collected nanotube networks. One reason may be, that treating the solution e.g. purifying or doping, is easier with using powder as the feedstock. However, collecting the nanotube network to a filter directly from the synthesis reactor is easier, or at least includes fewer steps. Basically the synthesis method, mentioned earlier, that you are using creates the nanotubes directly as a random dispersion to a filter, that is located at the end point of the reactor. The collection temperature, i.e. the temperature of the filter holder, is near room temperature. This provides a large usage of different filter types and materials. The filter material should be chosen keeping an eye on the future modifications that are planned to be done for the SWCNT network. The density of the SWCNT network on the filter can be easily controlled by controlling the collection time from the reactor and the synthesis temperature. The SWCNT network can be directly deposited to a transparent and flexible substrate, usually a polymer of some kind. This can be done in several ways, such as dry printing, electrical or thermal precipitation and thermo compression process that is used in the NanoMaterials Group.

Both of the above mentioned SWCNT thin film fabrication processes usually include some modification, to enhance the properties, of the network either with chemical or physical processing [33].

10 Processes for fabricating devices made from CNT networks

SWCNT thin films possess qualities that are useful in many possible applications such as light-emitting diodes, transistors, filters, field emitters, flat panel displays, touch screens and photovoltaic devices to mention a few [33]. Processes for fabricating these applications are yet to be fully developed. However, requirements for the material is that it should have low power consumption, high sensitivity, mechanical and chemical stability, flexible transparent substrates, flexible transparent interconnects and it should be mass producible at low cost [34]. The properties in sheet resistance and transparency should also at least match the properties of the current choice of material, ITO. However as ITO is expensive material, as a consequence of poor availability of indium, and depositing ITO requires high temperature and vacuum conditions, SWCNTs with matching qualities are considered as replacement for ITO [28]. The next section briefly approaches the fabricating methods and common properties.

Recent studies have shown that a SWCNT thin film can act as a conducting channel in field effect transistors (FET) and more importantly the thin film transistor (TFT) version of the FET [35]. It has been shown that low density SWCNT networks act as *p*-type semiconductor, and has field-effect mobility an order of magnitude larger than materials used in commercial TFTs [35]. A schematic of a typical TFT is shown in figure 13.
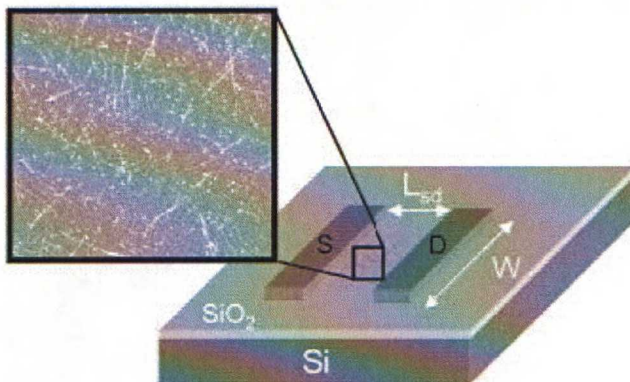

Figure 13. Typical schematic of a thin film transistor (TFT) [35].

The SWCNT thin film is grown on a thermal oxide substrate (SiO$_2$), the source and drain electrodes are fabricated using optical lithography and lift-off. The other regions are protected by a photo resist and SWCNTs from other areas are removed. The length of the source – drain channel determines the type of the conductivity. If the channel length is short, individual SWCNTs are long enough to provide conductivity from source to drain. If the channel length is longer than the length of individual SWCNTs, the percolation threshold gives the density, at which the network is conducting from source to drain. These examples make the network act like a metallic conductor, thus the off-state current is high. This means that the density of the network has to be carefully chosen so, that no such metallic pathways are formed. Thus the transistor applications need a network that has all the conducting pathways including semiconducting tubes [35].

Transparent and flexible transistors are a different kind of FETs that are the high end of the so called plastic electronics. SWCNTs can similarly be used as the conducting channel as mentioned. The fabrication of the transparent and flexible SWCNT transistor is described in detail by Artukovic et al. in reference 36. Briefly, the devices are prepared on a sheet of polyester. First a suspension of SWCNTs was sprayed on to the polyester substrate to from a dense nanotube network. Figure 14 shows a schematic of the transistor from reference 36
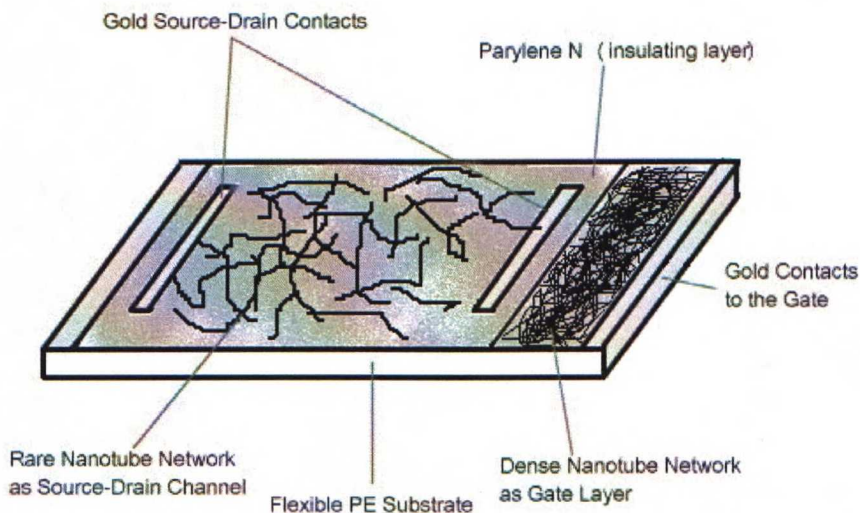

Figure 14. Schematic of a flexible and transparent SWCNT transistor.

The dense SWCNT network can be seen as the gate layer in the figure. A parylene N layer is deposited as the insulating layer of the transistor. A similar suspension with a lower SWCNT concentration is prepared and adsorbed to the parylene N by depositing the solution drop by drop to achieve the wanted density. The rare network acts as a source – drain channel in the transistor scheme as can be seen in figure 14. Gold contacts are evaporated to the network to form the source and the drain [36].

SWCNTs have also been planned to use and researched as a transparent and flexible sensors [34]. The fabrication of the transparent SWCNT thin film is described in detail in reference 32. Briefly, a dispersion of SWCNTs is prepared with a wanted concentration. The dispersion is then vacuum filtered through an alumina filter, and the SWCNTs attach to the filter as a SWCNT network. The density of the network can be controlled with the concentration of the dispersion and the filtrated volume [32]. To get the SWCNT network from the alumina filter to the transparent and flexible substrate, a polydimethysiloxane (PDMS) stamping method is used. First the network is attached to the PDMS substrate by simple adhesion and mild heating, and after that the PDMS substrate can be used as a stamper to stamp the network on to the transparent and flexible substrate [32 and 34]. In reference 34, the transparent and flexible sensor was used for NH_3 sensitivity testing. The sensing occurs as a decrease or increase in the SWCNT thin film conductance. The effect of NH_3 adsorption to the SWCNT energy band is believed to be a consequence of electron donation of NH_3 that raises the Fermi level and reduces the hole concentration. Also the NH_3 is believed to increase the local scattering of holes and therefore reduce the carrier mobility. It is also believed that lower SWCNT concentration on the thin film increases the sensitivity [34]. SWCNT thin films are planned to be used as sensors and biosensors in the future, with exploitation of measurable changes in conductivity.

Transparent SWCNT thin films are also been considered as a replacement of ITO, or other similar transparent conductive oxide (TCO) such as ZnO, in solar cells and other organic and inorganic photovoltaic devices [37 and 38]. The organic solar cells are considered a promising low-cost alternative to the usual silicon solar cells available commercially. The fabrication of such device, where the transparent electrode ITO is replaced by a transparent SWCNT thin film, is explained in detail in reference 38. Briefly, the SWCNT thin films are a replacement of ITO for hole collection. First,

SWCNTs are deposited from a solution with desired density on a glass substrate. The solar cells are prepared from a solution of poly(hexyl)thiophene-[6-6]phenyl-C_{61}-butric acid methyl ester (P3HT-PCBM) in chlorobenzene. A layer of poly(ethylenedioxy)thiophene:poly(styrene) sulfonate (PEDOT:PSS) is spin coated on to the SWCNT-glass substrates. Gallium-indium eutectic was used for the contacts of the SWCNT and the P3HT:PCBM layer. A schematic of the device is in figure 15. Figure 15 also shows the reference device using ITO as the electrode, as it can be seen the SWCNT are simply a replacement for ITO in the device structure [38].
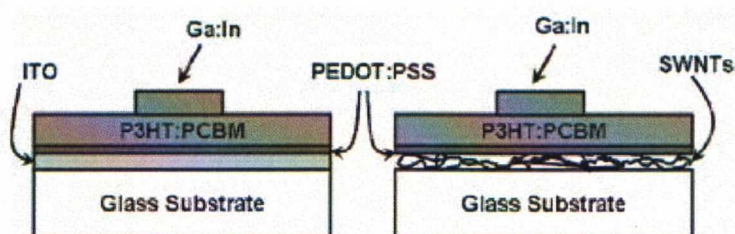

Figure 15. A schematic of an organic solar cell

One example of inorganic photovoltaic device is introduced in reference 37. The device consists of SWCNT/CdS/CIGS/Mo/Glass layers. The CIGS absorber is grown onto the molybdenum coated glass by evaporation from elemental sources. The CdS is deposited by chemical-bath deposition. Finally the device is coated with a thin layer of SWCNTs. The device does not have the same efficiency values that with using a TCO, but then again it is not yet optimized. However it is shown that the transparent SWCNT thin films have a higher transmittance in infrared (IR) wavelengths than the most usual TCOs, an important aspect considering photovoltaic devices [37].

Perhaps the most intriguing application for SWCNT thin films is flat panel displays (FPD). In this context, FPDs can be thought to be for example computer displays, cell phone displays, foldable displays and flat screen TVs. These devices have a huge worldwide market behind them and the replacement need of the rare and brittle material indium, in the form of ITO in displays, has accelerated the development of new kind of displays. SWCNTs are used as field emitters in field emission displays (FED), or as a transparent electrode as ITO in conventional FPDs such as liquid crystal displays

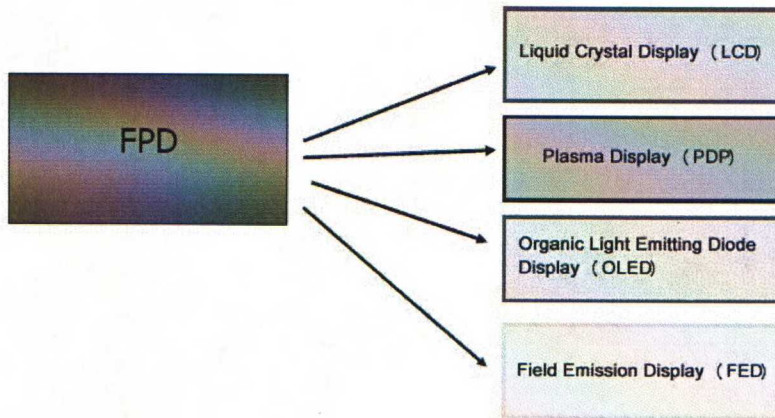(LCD) and plasma displays (PDP) [5]. Figure 16 show four of the main different kind of FPD technologies.

Figure 16. Four different techniques for flat panel displays.

In the FEDs, aligned arrays of CNTs are used as emitters in a similar way that cathode ray tube (CRT) displays. FEDs just have multiple "cathode rays", CNTs that is, behind every pixel. Because this thesis is focused on transparent SWCNT thin films, the FEDs won't be considered here in detail. For other type of displays SWCNT thin films are used as a transparent conductor such as TCO thin films are used [13]. Not much research has been published about flat panel displays that are manufactured using a SWCNT thin film as a transparent conductor, FEDs are in that way more researched, in public anyway. However if we get a little deeper on fabrication techniques of FPDs using ITO or other TCO, we can see where the SWCNT thin films fit in that picture.

Each FPD technology is using different kind of thin film architecture and each of them requires unique specifications for layers and manufacturing process steps. This means for TCOs and SWCNT thin films a specific tailoring for deposition of the thin film and post-deposition process. In LCD technology for instance, the back light has to travel through two transparent electrodes, which operate as electronic directors for the liquid crystal, as seen in figure 17. In figure 17, which represents the typical cross-section of a LCD, the ITO electrode can be thought as SWCNT thin film instead [39].
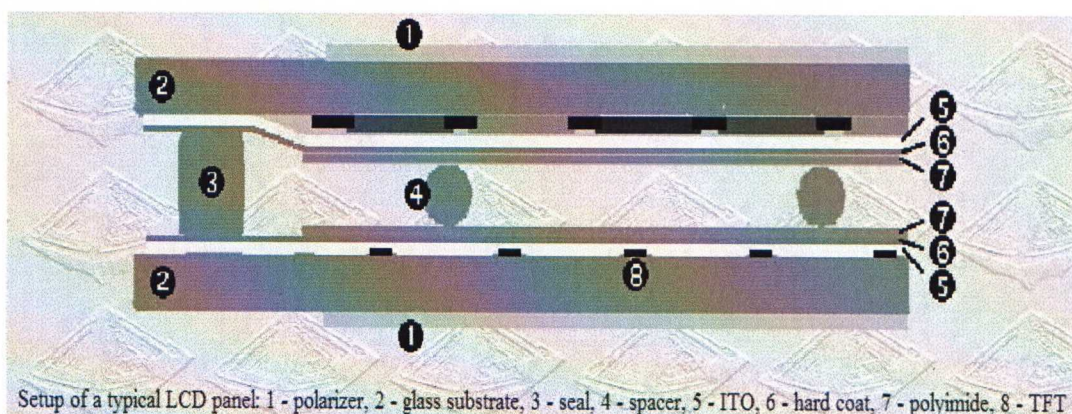
31

Setup of a typical LCD panel: 1 - polarizer, 2 - glass substrate, 3 - seal, 4 - spacer, 5 - ITO, 6 - hard coat, 7 - polyimide, 8 - TFT

Figure 17. Cross-section of a typical LCD panel setup.

The requirements for a SWCNT thin film acting as the transparent electrode in a setup seen in figure 17, include a transparency of 90 % or higher and a resistivity of $1\text{–}3\cdot10^{-4}$ $\Omega\cdot$cm. For PDPs, TCOs are used in a similar way that in LCDs. PDPs consist of three electrodes and a dielectric layer, as can be seen in figure 18.
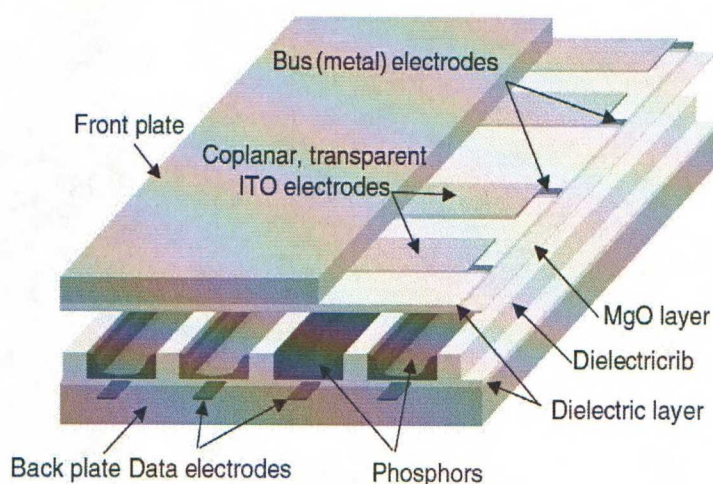
Figure 18. Schematic of a typical PDP panel setup.

The transparent electrodes, where SWCNTs thin films are used in the future, are seen as ITO electrodes in figure 18; just behind the front plate of the display. PDPs have size criteria due to Paschen´s rule. T. Suzuki states in reference 40, that "the Paschen´s rule establishes a limit on minimum electrode gap distance for glow discharge at a filling gas pressure." In reality, this means that PDPs cannot be scaled down under 30 inch screen size [40].

Besides FEDs, a new display technique is being developed to decrease the thickness, response time and power consumption of conventional displays. Organic light emitting diode (OLED) displays are especially planned for future flexible displays [39]. In OLED displays, SWCNT thin films would work as an anode in the two electrode composition as seen in figure 19, where the anode is represented by ITO.
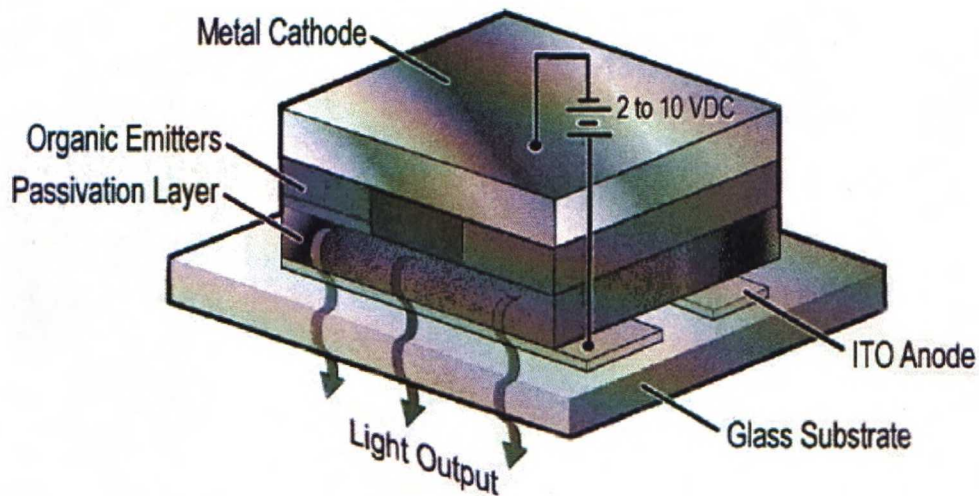
Figure 19. A simplified cross-section of a typical OLED display setup.

For the transparent anode in OLED displays, the specifications are a high work function and an ultra smooth thin film surface [39].

The transparent electrodes in different FDP techniques are deposited to the substrates by sputtering methods (ITO) or by the methods described in chapter 9. Patterning can be made by using standard photolithography or other printing methods mentioned in chapter 9, and in reference 32 [32 and 39].

11 Methods

The starting point of the thesis was to create a transparent, conducting and flexible carbon nanotube thin film. The properties of the film considering the transparency and conductivity should get as close as possible to the published values of other CNT research groups and TCOs used in commercial applications. The flexibility of the thin film should be shown by unchangeable properties after bending. Theories to conductivity and transparency should be discussed and shown considering the manufacturing methods at NMG. This chapter describes how the samples used in the measurements are prepared, modified and treated in order to get the wanted results.

11.1 Fabrication the sample

The SWCNTs were produced using the ferrocene decomposition method described in chapter 7, in a laminar flow reactor. Thus, ferrocene was used as catalyst nanoparticles and as a carbon source. CO (99, 97 vol%, AGA) was used as a carrier gas and it also served as a precursor for the synthesis. The total flow rate of CO, consisting of saturation and additional flow rates (300 and 110 cm^3/min) was 410 cm^3/min. The ferrocene was introduced to the reactor 7,5 cm from the reactor furnace inlet. The injector probes which were used to feed the precursor to the furnace were held at 22 °C. The constant partial pressure of the precursor was 0,8 Pa. The SWCNTs grow from the iron nanoparticles, i.e. they act as the formation sites for the tubes. The diameter of the nanoparticles determines was strongly correlated to the diameter of the nanotubes with a ratio of 1,6 [41]. The diameter of the SWCNTs collected with this method varies between 0,9 nm to 3 nm. The SWCNTs were collected to a 25mm diameter filter (Millipore Corp., USA) that was located at the outlet of the reactor in a special filter holder. The filter material can be chosen freely. The temperature in the filter holder was estimated at 45 °C. One end of the filter holder was attached to a vacuum line which had a flow rate of 280 cm^3/min, and the other end was attached to the reactor. As soon as the filter holder was attached, the SWCNT were being collected to the filter. When the collection time was up, collection time can be chosen freely, the filter holder was detached from the reactor and then detached from the vacuum line. When the filter

holder was opened, you had a filter with SWCNTs and you were ready to continue with further processing steps. The SWCNTs collected to the filter were readily in the form of SWCNT network, which consists largely of small bundles of SWCNTs. The filter holder was cleaned after each collection. Temperature, collection time, carrier gas, filters material and the date were recorded. Figure 20 shows a picture of the stainless steel filter holder, an empty nitrocellulose (NC) filter, and a filter with SWCNT network on it. The collection time for this particular sample was 30 minutes and the synthesis temperature was 1000 °C.

Figure 20. Stainless steel filter holder, with an empty filter on it and a CNT network collected to a filter.

The properties of the SWCNT network can be altered by changing the temperature of the synthesis and by varying the collection time. The DMA system attached to the reactor allows measuring the electrical mobility of the particles and thus provides the catalyst particle aggregates from the SWCNT bundles. This also correlates especially to the electronic properties of the network.

11.2 Modification of sample properties

The untreated pristine samples collected from the reactor, rarely give the results that are wanted. In order to achieve the wanted properties, modifying of the samples was needed. As stated earlier many modification methods are been used by

research groups and different kind of results have been achieved. Here will be presented the modifications that were made to our SWCNT networks. Note that all the modifications were not made to the same sample, i.e. one sample may be modified with just one treatment or multiple treatments.

11.2.1   Sputtering

The SWCNT networks located at the filter were sputtered with metal particles in an attempt to achieve a lower sheet resistance of the sample. The idea behind the sputtering was to sputter the metal particles to the junctions of SWCNT bundles to achieve better conduction between the junctions. A special sputter coater device was used. The target metal was placed and located at the top of the sputtering chamber. The sample was put on the sample plate located at the low end of the sputtering chamber. The sputtering conditions were chosen and mainly the sputtering current and sputtering time were adjusted. Figure 21 shows the sputtering device (Agar, England) used for our experiment.

Figure 21. The sputtering device with the chamber on the left side of the device.

Before the sputtering begun a correct atmosphere was set by flushing the chamber so that maximum value was achieved. The sputtering takes place in argon (Ar) atmosphere. The metal particles were thus bombarded with Ar ions to the surface of the sample. The target metals used were gold (Au), iron (Fe) and platinum (Pt). After the sputtering, the

36

sputtering chamber is set to normal atmosphere using the leak setting, before it can be opened and the sample removed.

11.2.2   Ethanol treatment

The ethanol treatment was usually applied to pristine samples that lie on the filter straight from the reactor. In ethanol treatment it was crucial to use a filter material that can withstand the effect of ethanol. The ethanol was applied with a standard plastic syringe, with a needle on the tip of it. Figure 22 shows the procedure in detail.
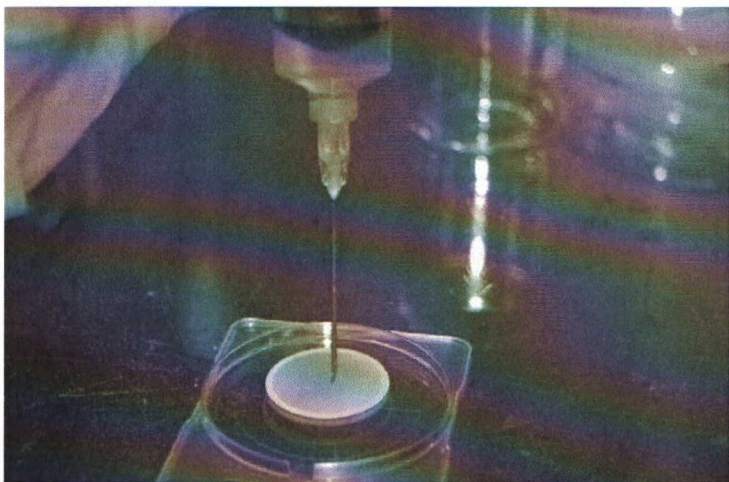
Figure 22. Applying ethanol to the CNT network with a syringe and a needle.

The syringe was filled with a fair amount of ethanol, and the air left to the syringe was blown out. Then the syringe was placed on top of the sample, and the sample was treated drop by drop until the ethanol covers the whole sample. Then the sample was left to dry.

11.2.3   Nitric acid treatment

The nitric acid treatment was usually applied to a sample that was already treated with ethanol. In nitric acid treatment, it was even more crucial to use a filter

material that can withstand the highly corrosive and toxic acid. The nitric acid was applied much in the same way as ethanol in figure 22. The nitric acid was applied drop by drop until the whole sample area was covered. Instead of plastic syringe, a glass syringe was used because of the corrosive nature of nitric acid. Because nitric acid was an aqueous solution, the filter must be placed so, that the acid can dry easily. A similar filter holder as used in the collection of the SWCNTs was used when applying the nitric acid. Because nitric acid was a strong corrosive acid, the treatment should be made in a fume hood. Protective clothes, lab coat, gas mask, rubber gloves and goggles, should be used. The sample must be dried properly before further steps can be made, and this may take even days.

11.3 Sheet resistance

The sheet resistance of the samples was measured straight from the filter with an easy one step process. The equipment used was a standard multimeter, with a special sheet resistance probe attached to it. The probe was Prostat's PRF-912B microprobe that is specially designed to measure sheet resistances on small samples. The probe used for the sheet resistance measurements is seen on figure 23.

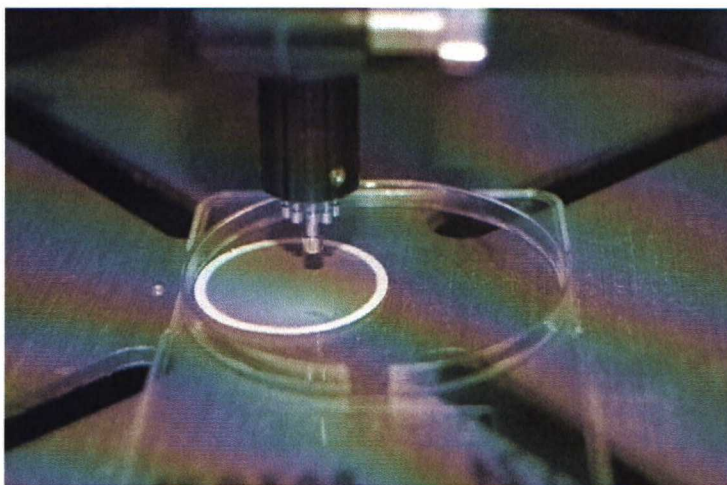
Figure 23. The sheet resistance measurement probe and the sample.

The probe consists of miniature concentric ring fixture with one miniature probe in the middle and ten miniature probes in a circle around the middle probe. The outer diameter

of the probe is 12,7 mm and the minimum contact diameter is 8,2 mm. The contact resistance between the metal probe and the SWCNT network was measured to be linear, thus the contact is ohmic. The sample is located at the table below the micro probe. The sheet resistance was measured with simply pulling down the probe using a lever where the probe is attached, pressing it until it reaches its down position so that all the miniature probes have contact with the surface. The probe was kept on the sample until the reading on the multimeter's display was fixed. The probe tips must be cleaned properly between every measurement, in case of nanotubes are attached to the probes.

11.4 Thin film deposition

In NMG a simple thermo-compression method is used to transfer the SWCNT network onto a polymer to form a conducting, transparent and flexible SWCNT thin film. The network was transferred to a medium density polyethylene (PE) polymer film (Metsä Tissue Ltd, Finland). The material was chosen, because it is highly transparent and flexible. The equipment used consists of a normal laboratory hot plate with adjustable temperature and a weight plate of 191,8 g that can be seen in figure 24.
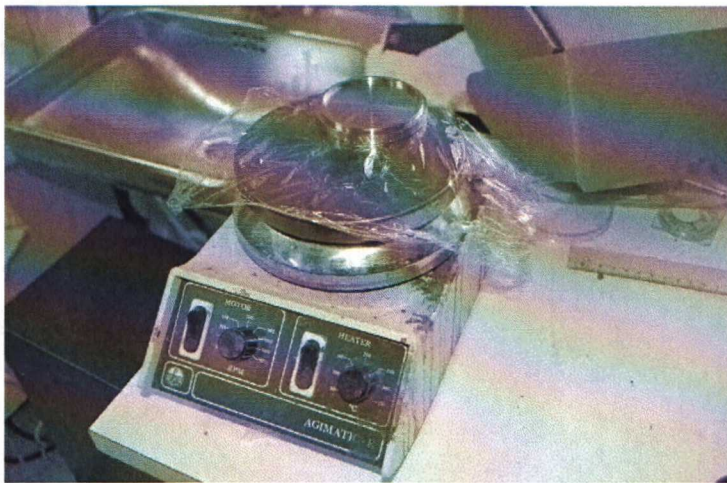

Figure 24. Equipment used depositing the CNT network on the PE polymer film.

The deposition of the SWCNT network was done fast by few easy steps. First the PE film was placed on to the hot plate, which was heated up to 100 °C. 100 C° is determined to be the best temperature for the deposition, because of the melting

39

temperature (125 °C) and the glass transition temperature (-125 °C) of the PE film. It is also the temperature where the PE film stays the most transparent [34]. The filter with SWCNT network was placed face down on the PE film located at the hot plate. The weight was put on the filter on the PE film, and it creates a pressure of 4,26 N/cm^2 The pressure was applied for 10 to 15 seconds, and after that the weight and the PE film are removed from the hot plate. After the PE film has cooled down, the filter was carefully removed and the SWCNT network had been completely transferred to the PE film to create a transparent SWCNT thin film.

11.5 Transparency

Transmittance measurements were used to measure the transparency of the prepared SWCNT thin films. Transmittance is defined as the fragment of light that passes through the sample at a certain wavelength. A UV/Vis/NIR (ultraviolet/visible/near infrared) spectrometer (PerkinElmer Life and Analytical Sciences, USA) was used. The spectrometer has a wavelength scale of 190 – 3200 nm with an integrating sphere of 190 – 3200. The integrating sphere performs a diffuse transmission through the sample, thus preventing possible errors caused by the refraction and light scattering of the sample. This way, the possible surface roughness of the sample can suppressed. The samples were measured using a reference sample, which was an empty PE film with no SWCNTs on it.

11.6 Imaging

The images of the SWCNT thin films and network were taken with electron microscopy or scanning probe microscopy. More precisely a scanning electron microscope (SEM), a transmission electron microscope (TEM) and an atomic force microscope (AFM) were used.

SEM is a type of electron microscopy, which can provide high resolution images of a sample surface. It is ideal for small area samples with providing a reasonable overview of the sample surface and dimension. In principle an electron gun is used to accelerate the electron towards the sample. The energy exchange between the

electrons and the sample, results in the emission of electrons and electromagnetic radiation, which results an image to be seen on the SEM screen. The SEM images are helpful in determining the properties of the SWCNT thin films and networks.

TEM is also type of electron microscopy which is highly used in imaging of small samples, like CNTs. It also uses electrons to produce images, but the electrons interact with the sample more than in SEM. The electrons pass through the sample, and use the diffraction to produce the image. The TEM is also installed with energy dispersive x-ray spectroscopy (EDS) which provides chemical characterization, e.g. elements present, of the sample.

AFM is a very high resolution type of scanning probe microscope (SPM). Its resolution goes as deep as fractions of nanometer, so naturally it is one of the key microscope techniques used in researching CNTs. The AFM uses a mechanical probe, i.e. a sharp tip, which scans through the surface of the sample. In principle a force, mechanical contact force, Van der Waals forces etc., between the sample and the probe provide the information required to form the image. An interesting point of AFM probes are, that CNTs are a novel probe material for the AFM.

11.7 Flexibility

The flexibility of the SWCNT films can be tested just by flexing the film and seeing what happens to the film. The flexing may have affect on the properties, though it looks the same after flexing. This can be tested, by testing the properties before flexing and after flexing of the SWCNT thin films. The flexibility of the network is a result of the networks spider web-like nature. The network consists of a web of nanosized wires, which gives it a lot more mechanical flexibility and strength over a uniform thin film [13].

41

12 Results

This chapter presents the results achieved in our research. Effect of modifications is examined and comparing to other results achieved by other research groups is presented. The results are mostly concentrating on sheet resistance and transparency, which are the key properties for SWCNT thin films.

12.1 Sheet resistance

The sheet resistance was measured using the setup described in previous chapter. This section approaches the affect of different process steps and conditions on sheet resistance.

12.1.1 Synthesis temperature

The effect of synthesis temperature, thus the temperature where the CNTs are formed in the gas phase, has a strong affect on the sheet resistance of the samples. Table 1 shows the measured sheet resistance for pristine samples collected for 30 minutes in different synthesis temperatures.

Table 1. The effect of synthesis temperature on sheet resistance.

Collection time (minutes)	Temperature (°C)	Sheet resistance ($\Omega/\square$)
30	1000	74500
30	850	8600
30	825	5850
30	800	12200
30	775	36000

Table 1 clearly shows the synthesis temperature dependence on the sheet resistance of the pristine SWCNT networks. The reason behind this correlation is that the individual CNTs and CNT bundles that form the network are longer and their diameter is smaller in temperatures below 900 °C [22]. As stated earlier in chapter 8, the length and diameter of the bundles have a strong correlation to the sheet resistance value, and our

research results confirm this. According to table 1, 825 °C seems to be the ideal synthesis temperature for SWCNT networks that require low sheet resistance.

Figure 25 shows a SEM image of a pristine sample that was collected for 25 minutes and the synthesis temperature was 825 °C.
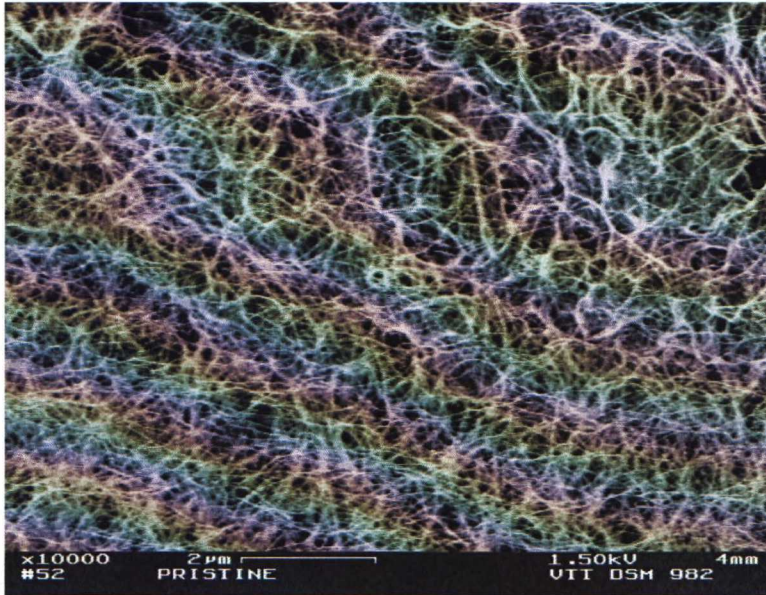

Figure 25. A SEM image of a pristine sample synthesized for 25 minutes in 825 °C.

The figure shows an overview image of the SWCNT network where the sparse nature of SWCNT networks is shown. The SWCNT bundles are seen as the white lines and bundles with a length of over a micron are seen.

12.1.2   Sputtering

Sputtering treating was done to the samples, in order to achieve metal particle coating for the junctions in the SWCNT networks. However the sheet resistance did not decrease after the sputtering treatment. Instead it remained almost the same or increased. Au, Fe and Pt sputtering yielded the same results and changing the sputtering time and current, did not give any better results. Table 2 shows the change of sheet resistance for every target metal used. The increase of the sheet resistance seen in table 2, can be due to deformation of the SWCNTs that occurs while the argon ions hit the surface of the samples.

Table 2. The effect of sputtering on sheet resistance.

Collection time (min)	Temperature (°C)	Target	Current (mA)	Sputtering time (s)	Sheet resistance Before (Ω/□)	After (Ω/□)
30	1000	Pt	10	10	74500	**250000**
20	1000	Pt	10	5	140000	**250000**
30	1000	Au	10	10	74800	**422000**
60	1000	Fe	10	5	85000	**100000**

Figure 26 shows a TEM image of the iron sputtered sample, and it shows the iron particles (black) on the SWCNT network. However, it is hard to say from the picture are the tubes damaged or not.

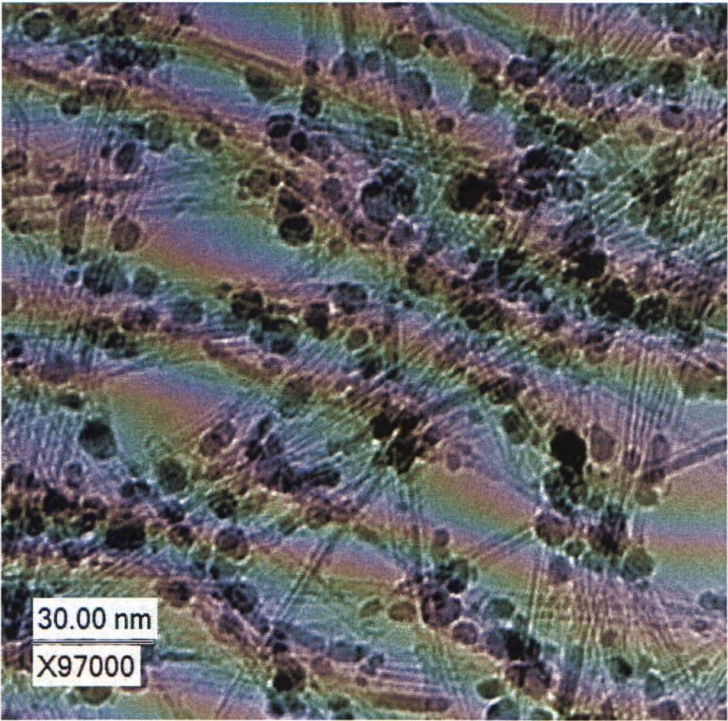Figure 26. A TEM image of a Fe sputtered SWCNT network

12.1.3   Ethanol treatment

SWCNT networks are usually modified chemically to achieve the wanted low sheet resistance. In our group the samples are usually treated with at least ethanol,

which has a big effect on the sheet resistance. Table 3 shows, how the applied ethanol treatment affects the sheet resistance of the SWCNT networks.

Table 3. Effect of ethanol treatment on sheet resistance.

Collection time (minutes)	Temperature (°C)	Sheet resistance	
		Pristine sample (Ω/□)	After ethanol (Ω/□)
30	1000	74500	1820
30	850	8600	702
30	825	5850	881
30	800	12200	965
30	775	36000	6700

Table 3 shows the significant change in sheet resistance of the ethanol treated samples. The ethanol treatment has a densifying effect on the samples, thus it makes the network more closely packed. Figure 27 shows a SEM image of an ethanol treated sample.
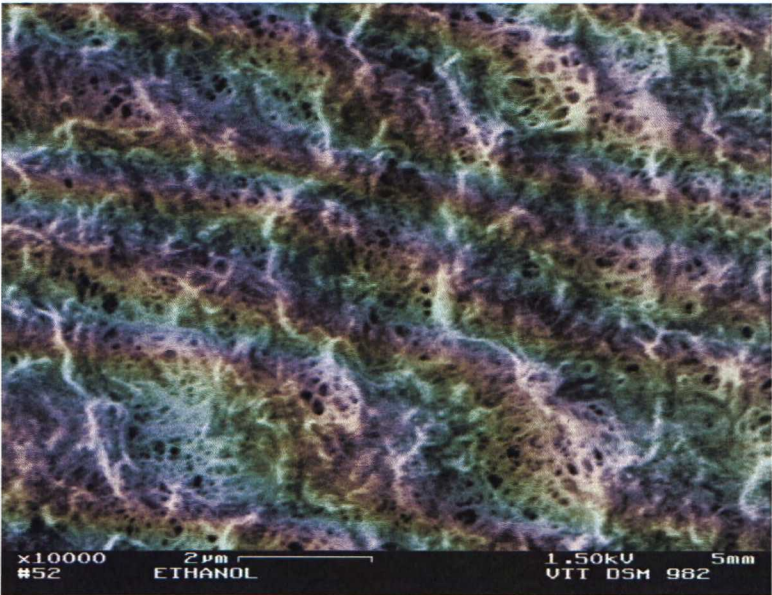

Figure 27. Ethanol treated SWCNT network.

The densifying effect of ethanol can be clearly seen from figure 27. The tubes are more closely packed and thus more conducting pathways are present. The SWCNT network in figure 27 was collected for 30 minutes and the synthesis temperature was 1000 °C. The synthesis temperature has clearly an effect on the length of the SWCNT bundles as they are much shorter than the bundles in figure 25. The density/thickness of the sample

synthesized in 1000 °C is clearly higher than the density/thickness of the sample synthesized in 825 °C as can be seen from figures 25 and 27. As stated earlier, the sheet resistance is highly dependent on the density of the SWCNT network, according to the percolation theory. Table 3 shows that densifying the sample decreases the sheet resistance by order of magnitude, so the density clearly has an effect on the sheet resistance of the SWCNT network.

12.1.4   Nitric acid treatment

Using nitric acid to modify the SWCNT network is a common preparation step in many research groups around the world. In our group however, the nitric acid is applied as described earlier and other groups using the solution deposit method, apply the nitric acid in the solution phase. The nitric acid treatment purifies the SWCNT network from amorphous carbon and leftover catalyst particles [26]. Nitric acid is applied after the ethanol treatment. The suitable filter material for nitric acid treatment was found to be polyvinylidene fluoride (PVDF). The nitric acid purification is the crucial step in modifying the samples. The sheet resistance values reached after the nitric acid treatment are comparable to published results from other research groups. Table 4 shows the decrease of the sheet resistance from pristine sample to nitric acid treated sample. It also shows the sheet resistance values for the ethanol treated samples, measured before the nitric acid treatment.

Table 4. The effect of nitric acid treatment on sheet resistance.

Collection time (min)	Sheet resistance		
	Pristine sample ($\Omega/\square$)	After ethanol ($\Omega/\square$)	After nitric acid ($\Omega/\square$)
45	2600	1250	250
30	8700	1600	340
25	8800	1700	430
20	8900	2700	590
15	12000	6700	790
10	21000	7500	1040

The samples in table 4 have been collected at different collection times, which will be discussed later. The synthesis temperature for the samples in table 3 was 825 °C, which was found to yield the best results as mentioned earlier.

12.1.5   Number size distributions

The aerosol mobility number size distributions (NSD) were measured in some of the collection occasions. The differential mobility analyzer (DMA) and a condensation particle counter (CPC) allowed us to measure the electrical mobility of particles, and to distinguish the geometric mean particle diameter. This diameter is correlated to the correct operation of the synthesis reactor [42]. This means, that it is correlated to the sheet resistance of the network. Table 5 shows the effect of the geometric mean particle diameter D_p, on the sheet resistance.

Table 5. The DMA measurements effect on sheet resistance

Geometric mean particle diameter	Sheet resistance ($\Omega/\square$)
100	200100
80	68000
70	74500

All the samples were collected for 30 minutes and synthesis temperature of 1000 °C. The samples are not modified in any way, thus the sheet resistance is high. The values just represent the meaning of the geometric mean particle diameter. Table 4 shows that when D_p = 80, the sheet resistance is the lowest of the measured values. It has been shown, that when the D_p = 80, the SWCNT network includes some inactive catalyst particles, which might contribute to the conductance [42]. However, it must be noted that the DMA measurements were not quantitative, because the DMA setup was not functional for a period of time. This may cause some variations between the measured samples, depending on the date they are collected.

12.1.6   Collection time

The collection time has an effect on the thickness, transparency and sheet resistance of the SWCNT sample. With just 45 minutes of collection time and nitric acid modification 250 $\Omega/\square$ sheet resistance value is achieved, as can be seen from table 4. The collection time and sheet resistance correlates almost linearly when the same synthesis conditions are used, which is presented in figure 28. The values for the figure are taken from table 4, so the samples used for the figure, are modified with ethanol and nitric acid.
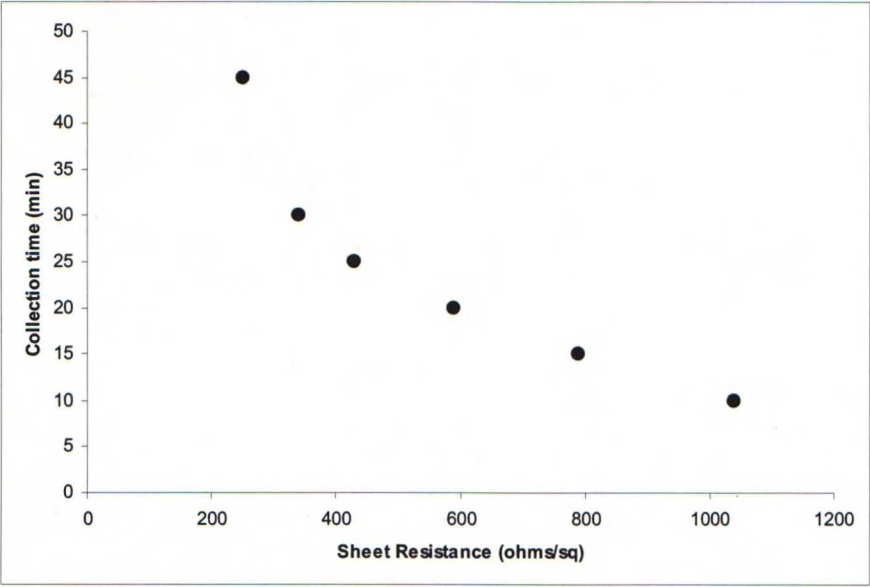
Figure 28. Correlation between collection time and sheet resistance.

12.1.7   Thin film deposition

When the pristine SWCNT networks are deposited to the PE film via thermo-compression, the sheet resistance of the samples is changing. Table 6 shows the effect of thermo-compression depositing on sheet resistance.

Table 6. Thin film depositing effect on sheet resistance

Sheet resistance	
Pristine sample ($\Omega/\square$)	Sample deposited on PE ($\Omega/\square$)
61500	18800
86500	15600
232000	24000

All of the samples are collected for 30 minutes and synthesis temperature of 1000 °C. The decrease in sheet resistance is due to densification of the SWCNT network while it is compressed. Figure 29 shows the as prepared SWCNT thin film.
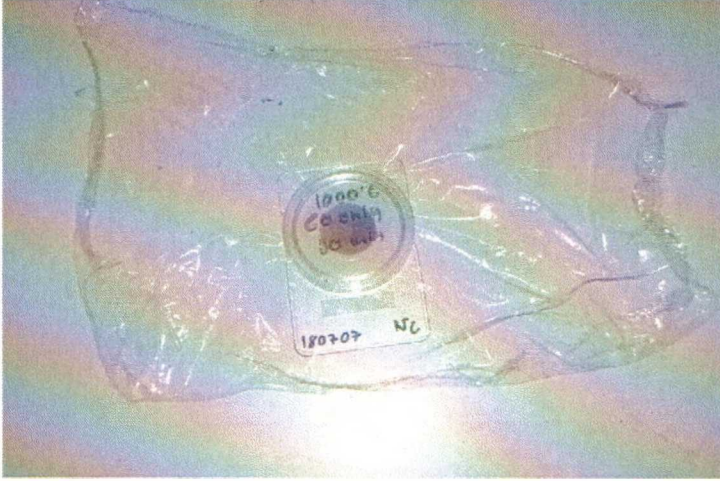
Figure 29. SWCNT thin film deposited on PE film with thermo-compression.

The thin film in figure 29 consists of a SWCNT network that was collected for 30 minutes in a synthesis temperature of 1000 °C and the transparency is estimated at 60 %. Figure 29 also shows the highly flexible nature of the thin film.

12.2 Percolation theory

As mentioned earlier, several groups have proved that standard percolation theory can be at least partly used to understand the conductivity of the SWCNT networks [26]. We have measured the thickness of our samples, so we can use equation 8, to estimate the critical exponent α for our samples. First, the equation has to be modified to give us the critical exponent α:

$$\sigma \approx (t - t_c)^{\alpha} \Rightarrow \ln \sigma = \alpha \ln(t - t_c) \Rightarrow \alpha = \frac{\ln \sigma}{\ln(t - t_c)} \tag{9}$$

The conductivity σ in equation 9, can be expressed as resistivity ρ, which is the reciprocal of conductivity i.e. $\rho = 1/\sigma$. The resistivity can be calculated with our sheet resistance and thickness values as $\rho = R_s \cdot t$. Thus the equation used in our calculations is:

$$\alpha = \frac{\ln\left(\dfrac{1}{R_s \cdot t}\right)}{\ln(t - t_c)} \tag{10}$$

The thickness of the samples was supposed to be evaluated by using AFM. However, the measurement was proven to be non-trivial due to some disturbing factors, and the thickness could not be estimated. To estimate the thickness we used a transmittance – thickness curve from our recent publication [33]. As we had the measured transmittance values for our samples, we could calculate the thickness values using the curve. Table 7 shows the process conditions for the used samples and table 8 shows the calculated thickness and critical exponent values for selected samples. The samples have been modified with ethanol and nitric acid.

Table 7. Process conditions for selected samples.

Collection time (min)	Synthesis Temperature (°C)	Transparency (%T)	Sheet resistance (Ω/□)
30	850	71,6	350
45	825	77,4	300
30	825	79,6	410
10	825	96,8	4400

Table 8. The thickness and critical exponent values.

Thickness (nm)	Critical exponent α
206	0,93
126	1,16
105	1,18
24	1,49

As SWCNT networks are considered to be 2D, the critical exponent due to percolation theory should be 1,33 as stated earlier in chapter 8. The critical exponents in table 8 are less than that, except for one. This suggests that a bigger decrease in sheet resistance can be achieved with either further or different kind of modification or doping of the samples, or by some other quality controlling methods during the synthesis.

12.3 Transparency

The transparencies of the samples were measured with the spectrometer using the method mentioned in chapter 11. This section approaches the process steps and conditions that affect the transparency of the sample. All of the transparencies measured are measured from pristine samples, because the thermo-compression deposition method did not work for modified samples because the SWCNT network

was highly attached to the filter after modification. The pristine samples were deposited to the PE film as described in chapter 12.

12.3.1   Collection time

The transparency is highly correlated to the thickness of the SWCNT network. The thickness on the other hand is strongly correlated to the collection time of the samples, if the samples are otherwise synthesized under the same conditions, e.g. temperature. Figure 30 shows the transmittance/transparency curves for three different collection times, 10, 30 and 45 minutes, synthesized in 825 °C. The heaving of the curves is due to the interference of the PE film.
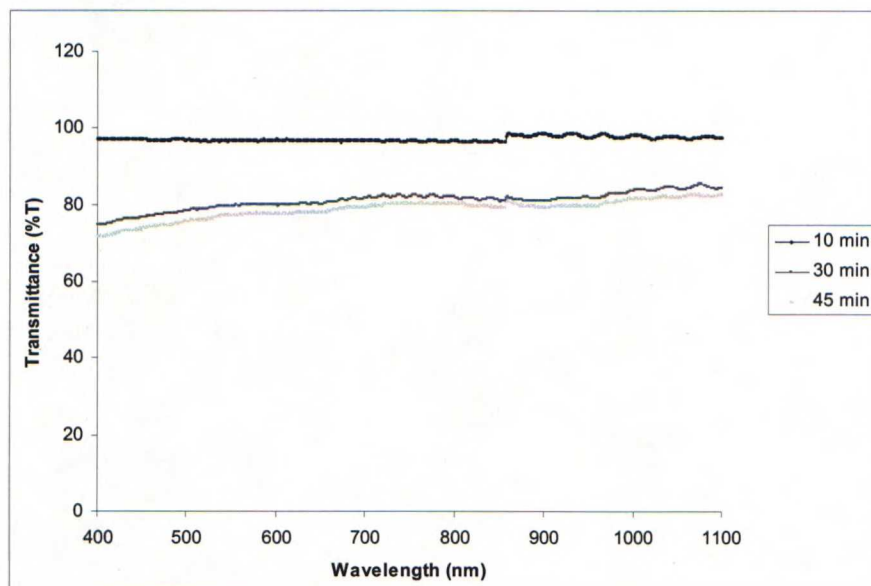

Figure 30. Difference in transparency between different collection times of the thin films.

From figure 30 the difference in transparency for different collection times can be seen. The transparency difference between samples remains almost the same from the visible light wavelengths to the near infrared wavelengths.

12.3.2   Synthesis temperature

The synthesis temperature has an effect on the transparency, as long as the collection time and other features remain same for the samples. Figure 31 shows the

51

transmittance/transparency curves for three samples synthesized in temperatures 1000 °C, 850 °C and 825 °C for 30 minutes.
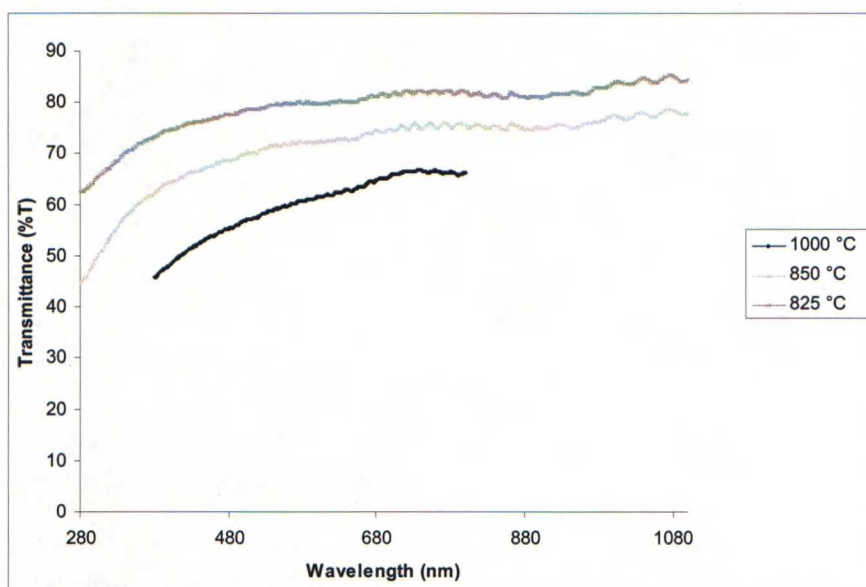

Figure 31. Synthesis temperature effect on transparency of the thin film.

The curve for the 1000 °C sample is shorter, because it was measured only in the visible light wavelengths. The difference in transparencies for different synthesis temperatures is clear according to figure 31. The difference can be explained with the different yield of CNTs from the reactor. The lower the temperature, the lower the yield of the CNTs. Thus the thickness of the samples varies with the yield of the CNTs. As thickness is correlated to the transparency, the transparency correlates with the yield of the CNTs as well.

12.3.3   Sheet resistance

A SWCNT thin film with a specific transparency value can have a wide range of sheet resistances depending on the state of the thin film. Various cases that affect the sheet resistance were presented in chapter 12.1. However these cases have no, or little, effect on the transparency of the thin film. Although the sheet resistance of the CNT networks is not directly correlated to the transparency of the network, results of researched samples are usually presented as transparency vs. sheet resistance graphs.

These represent the most important properties of CNT thin films, and so it is natural to present them together. The process conditions and results for the samples that were measured are found in table 7, presented in previous chapter. The transparency value in table 7 is a transmittance value at 550 nm wavelength, which is the wavelength usually used to describe the transparency in visible light. The samples in table 7 are modified with ethanol and nitric acid. The transparency was measured from the pristine sample before modification, because deposition to the PE film was not possible after modification as stated above. Figure 32 presents a transparency vs. sheet resistance curve for samples from table 7. The filter which held the sample was cut in half and the other part was modified and the other part was deposited to the PE film. Sheet resistance and transmittance were then measured.
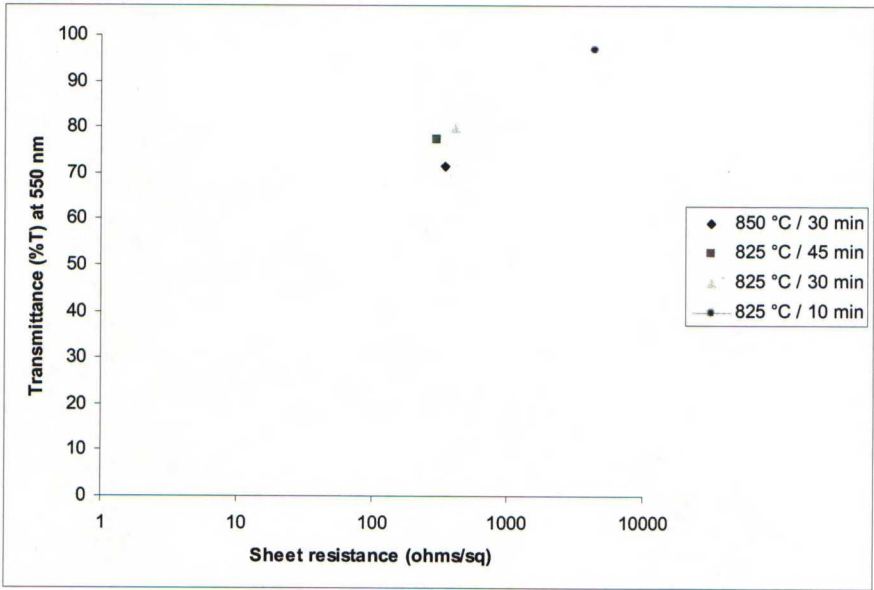

Figure 32. Transmittance at 550 nm vs. sheet resistance.

The results seen in figure 32 show a correlation between the sheet resistance and transparency. The data point that yields the lowest transparency is synthesized in 850 °C and the other data points are synthesized in 825 °C. These points show, that if the samples are created under similar conditions, the transparency is in fact correlated to the sheet resistance.

12.4 Flexibility

The flexibility of the prepared SWCNT thin films was tested qualitatively by measuring the sheet resistance before and after the flexing. Figure 33 shows how the sheet resistance changed during flexing.
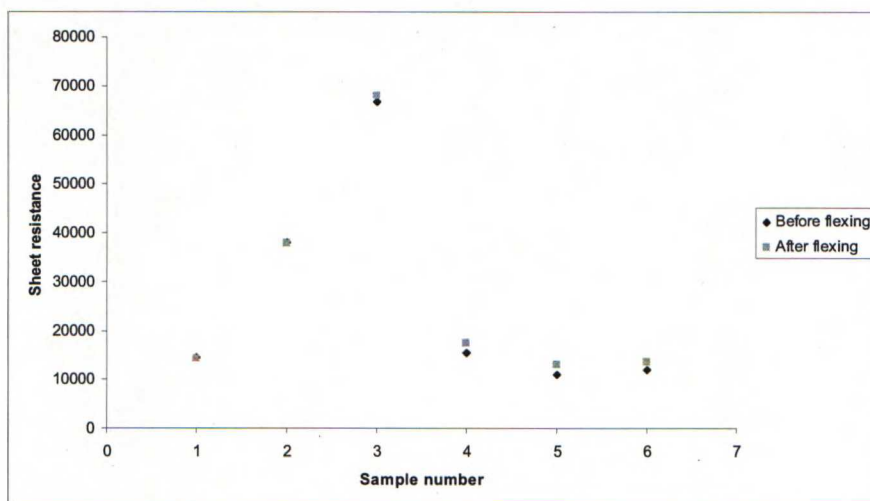

Figure 33. Changes in sheet resistance after flexing the sample.

The samples measured were unmodified SWCNT thin films deposited on PE film using the method described in chapter 11. The flexing of the sample was done by crumpling the sample between fingers for a while as seen in figure 34.

Figure 34. Crumpling of the SWCNT thin film.

This is a harsh method to test the sample, and applications usually just need flexibility of 180° or little twisting. In this light, the flexibility test was a success, as the sheet resistance does not vary a lot and the film remains whole as observed by eye after the test.

12.5 Patterning

The SWCNT network can be deposited as a patterned form on the PE film. This requires a use of special patterned filter when collecting SWCNTs from the reactor. The filter has a patterned figure, and the SWCNTs flowing from the reactor attach to this pattern. The filter material used in our experiment was made of polytetrafluoroethylene (PTFE), commonly known as Teflon™. The deposition of the patterned SWCNT network is carried out in the same way as normal networks. Figure 35 shows the patterned SWCNT thin film deposited on to a transparent PE film.
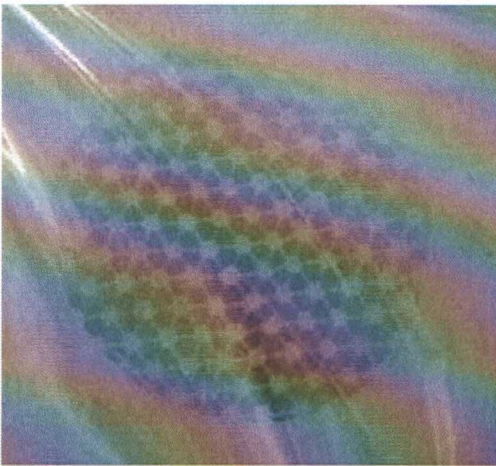

Figure 35. A patterned carbon nanotube thin film, deposited on polyethylene.

The figure shows, that patterning is relatively easy by using the right kind of filter material and the thermo-compression deposition method. The patterning property of the thin films is a step forward to printable electronics, where electronic circuits are patterned to flexible substrates.

13 Conclusions and discussion

The goal for this thesis was to create a conducting, transparent and flexible carbon nanotube thin film. The synthesis of the carbon nanotubes were made via ferrocene decomposition method and several different modifications to the pristine samples were made. The electronic properties of the CNT samples were tested after each modification step and analyzed.

The results received were encouraging comparing them to the published results from other research groups. The modification steps were evaluated based on the sheet resistance results they yielded. The best combination of modifications was the use of ethanol and nitric acid applied to the sample one after another. This yielded comparable results for CNT networks researched by other groups and for other TCOs such as ITO.

The percolating theory was tested for samples that were modified with ethanol and nitric acid. The critical exponent achieved was in average lower than the theory predicts. This gives us a clear indication, that the sheet resistance of our samples can be significantly lower. The lowering of the sheet resistance could be achieved with other modification steps that we have not tried yet, or just simply by gathering more information on the conductivity of the films by testing them more quantitatively.

The transparencies of the films were evaluated with different synthesis parameters and expected transmittance curves were achieved. The transparency was found to be dependent on the collection times of the samples and the synthesis temperature. Both of these affect the thickness/density of the sample, which correlates with the transparency.

The downside of the work done for the thesis was that the deposition to the PE film did not succeed after the samples had been modified with ethanol and nitric acid. To improve the adhesion between the modified SWCNT network and PE polymer film, in order to use the thermo-compression deposition method, is an important task for future work.

The future work in the SWCNT thin film electronics area concentrates mainly on the electronic properties of the thin films. Understanding the conductivity of the SWCNT network in theory and what affects it, is a crucial key to commercial thin

films. Considering commercializing, the manufacturing process must be able to produce large amounts of identical products with low cost. In some estimates FPDs use carbon nanotube technology in about 5 years.

References

1. Sumio Ijima. (1991). Helical microtubules of graphitic carbon. *Nature*. **354**. 56.
2. S. V. Rotkin, S. Subramoney (Eds.). (2005). Applied Physics of Carbon Nanotubes: Fundamentals of Theory, Optics and Transport Devices. New York: Springer Berlin Heidelberg.
3. J. W. Mintmire, B. I. Dunlap and C.T. White. (1992). Are fullerene tubules metallic? *Physical review letters*. **68**. 631.
4. G. Overney, W. Zhong and D. Tomanek. (1993). Structural rigidity and low frequency vibration modes of long carbon tubules. *Zeitschrift für Physik D*. **27**. 93.
5. Ray H. Baughman, Anvar A. Zakhidov and Walt A. de Heer. (2002). Carbon nanotubes – The route toward applications. *Science*. **297**. 787.
6. Yahachi Saito. (1999). Preparation an properties of carbon nanotubes. *Paper presented in IEEE International symposium on micromechatronics and human science*. 43.
7. J. W. Mintmire and C.T. White. (1995). Electronic and structural properties of carbon nanotubes. *Carbon*. **33**. 893.
8. Chunyu Li and Tsu-Wei Chou. (2003). A structural mechanics approach for the analysis of carbon nanotubes. *International journal of solids and structures*. **40**. 2487.
9. M. S. Dresselhaus, G. Dresselhaus and R. Saito. (1995). Physics of carbon nanotubes. *Carbon*. **33**. 883.
10. Hongjie Dai. (2002). Carbon nanotubes: Synthesis, integration and properties. *Accounts of chemical research*. **35**. 1035.
11. Lu-Chang Qin, Xinluo Zhao, Kaori Hirahara, Yoshiyuki Miyamoto, Yoshinori Ando and Sumio Iijima. (2000). The smallest carbon nanotube. *Nature*. **408**. 50.
12. L. X. Zheng, M. J. O'Connel, S. K. Doorn, X. Z. Liao, Y. H. Zhao, E. A. Akhadov, M. A. Hoffbauer, B. J. Roop, Q.X. Jia, R. C. Dye, D. E. Peterson, S. M. Huang, J. Liu and Y. T. Zhu. (2004). Ultralong single-wall carbon nanotubes. *Nature materials*. **4**. 673.
13. George Grüner. (2006). Carbon nanotube films for transparent and plastic electronics. *Journal of materials chemistry*. **16**. 3533.
14. J. - P. Salvetat. J. - M. Bonard, N. H. Thompson, A. J. Kulik, L. Forro. W. Benoit and L. Zuppiroli. (1999). Mechanical properties of carbon nanotubes. *Applied physics A. Materials science & processing*. **69**. 255.
15. Rudolf Steiner and ASM. (1990). Metals Handbook: Volume 1: Properties and selection: irons, steels and high-performance alloys (10th ed.). Materials Park, OH: ASM International.
16. Melissa Paradise and Tarun Goswami. (2007). Carbon nanotubes – Production and industrial applications. *Materials and design*. **28**. 1477.
17. Savas Berber, Young-Kyun Kwon and David Tomanek. (2000). Unusually high thermal conductivity of carbon nanotubes. *Physical review letters*. **84**. 4613.
18. J. Hone, M. Whitney, C. Piskoti and A. Zettl. (1999). Thermal conductivity of single walled carbon nanotubes. *Physical review B*. **59**. 2514.
19. M. Kaempgen, G. S. Duesberg and S. Roth. (2005). Transparent carbon nanotube coatings. *Applied surface science*. **252**. 425.

20. Teri Wang Odom, Jin-Lin Huang, Philip Kim and Charles M. Lieber. (1998). Atomic structure and electronic properties of single-walled carbon nanotubes. *Nature.* **391**. 62.

21. Phaedon Avouris, Joerg Appenzeller, Richard Martel and Shalom J. Wind. (2003). Carbon nanotube electronics. *Proceedings of the IEEE.* **91**. 1772.

22. Anna Moisala, Albert G. Nasibulin, David P. Brown, Hua Jiang, Leonid Khriatchev and Esko I. Kauppinen. (2006). Single-walled carbon nanotube synthesis using ferrocene and iron pentacarbonyl in a laminar flow reactor. *Chemical engineering science.* **61**. 4393.

23. Albert G. Nasibulin, Anna Moisala, David P. Brown, Hua Jiang and Esko I. Kauppinen. (2005). A novel aerosol method for single walled carbon nanotube synthesis. *Chemical Physics Letters.* **402**. 227.

24. Paula Queipo, Albert G. Nasibulin, Hua Jiang, David Gonzalez and Esko I. Kauppinen. (2006). Aerosol catalyst particles for substrate CVD synthesis of single-walled carbon nanotubes. *Chemical vapour deposition.* **12**. 364.

25. Elena Bekyarova, Mikhail E. Itkis, Nelson Cabrera, Bin Zhao, Aiping Yu, Junbo Gao and Robert C. Haddon. (2004). Electronic properties of single-walled carbon nanotube networks. *Journal of the American Chemical Society.* **127**. 5990.

26. L. Hu, D. S. Hecht and G. Grüner. (2004). Percolating in transparent and conducting carbon nanotube networks. *Nano Letters.* **4**. 2513.

27. L. Hu, G. Grüner, Dan Li, Richard B. Kaner and Jiri Cech. (2007). Patternable transparent carbon nanotube films for electrochromic devices. *Journal of applied physics.* **101**. 016102.

28. George Grüner. (2006). Two-dimensional carbon nanotube networks: A transparent electronic material. *Materials research society symposium proceedings.* **905E**. 0905-DD06-05.1.

29. David Hecht, Liangbing Hu and Geroge Grüner. (2006). Conductivity scaling with bundle length and diameter in single walled carbon nanotube networks. *Applied physics letters.* **89**. 133112.

30. Dietrich Stauffer and Amnon Aharony. (1994). Introduction to percolation theory. Taylor & Francis Ltd. London.

31. Axel Schindler, Jochen Brill, Norbert Fruehauf, James P. Novak and Zvi Yaniv. (2006). Solution-deposited carbon nanotube layers for flexible display applications. *Physica E.* **37**. 119.

32. Yangxin Zhou, Liangbin Hu and George Grüner. (2006). A method of printing carbon nanotube thin films. *Applied physics letters.* **88**. 123109.

33. Albert G. Nasibulin, Andrei Ollikainen, Anton S. Ansimov, David P. Brown, Peter V. Pikhitsa, Silja Holopainen, Jari S. Penttilä, Panu Helistö, Janne Ruokolainen, Mansoo Choi and Esko I. Kauppinen. (2007). Integration of single-walled carbon nanotubes into polymer films by thermo-compression. *Chemical engineering journal.* (In press). DOI: 10.1016/j.cej.2007.04.033.

34. Chang-Seung Woo, Yoon-Sun Hwang, Chae-Hyun Lim and Seung-Beck Lee. (2006). Highly flexible and transparent single wall carbon nanotube network gas sensors fabricated on PDMS substrate. *CKC Symposium, University of cambridge.*

35. E. S. Snow, J. P. Novak, P. M. Campbell and D. Park. (2003). Random networks of carbon nanotubes as an electronic material. *Applied physics letters.* **82**. 2145.

36. E. Artukovic, M. Kaempgen, D. S. Hecht, S. Roth and G. Grüner. (2005). Transparent and flexible carbon nanotube transistors. *Nano letters*. **5**. 757.
37. M. Conteras, T. Barnes, J. van de Lagemaat, G. Rumbles, T. J. Coutts, C. Weeks, P. Glatkowski and J. Peltola. (2006). Application of single wall carbon nanotubes as transparent electrodes in Cu(In, Ga)Se$_2$-Based solar cells. *Paper presented at the 2006 IEEE World conference on photovoltaic energy conversion*. Waikoloa, Hawaii.
38. Aurelien Du Pasquier, Husnu Emrah Unalan, Aloik Kanwal, Steve Miller and Manish Chhowalla. (2005). Conducting and transparent single-wall carbon nanotube electrodes for polymer-fullerene solar cells. *Applied physics letters*. **87**. 203511.
39. U. Betz, M. Kharrazi Olsson, J. Marthy, M. F. Escolá and F. Atamny. (2006). Thin films engineering of indium tin oxide: Large area flat panel displays application. *Surface & coating technology*. **200**. 5751.
40. Toshiharu Suzuki. (2005). Flat panel display – Impurity doping technology for flat panel displays. *Nuclear instruments and methods in physics research B*. **237**. 395.
41. Albert G. Nasibulin, Peter V. Pikhitsa, Hua Jiang and Esko Kauppinen. (2005). Correlation between catalyst particle and single-walled carbon nanotube diameters. *Carbon*. **43**. 2251.
42. Anna Moisala, Albert G. Nasibulin, Sergei D. Shandakov, Hua Jiang and Esko I. Kauppinen. (2005). On-line detection of single-walled carbon nanotube formation during aerosol synthesis methods. *Carbon*. **43**. 2066.